Underthrusting and exhumation: A comparison between the External Hellenides and the "hot" Cycladic and "cold" South Aegean core complexes (Greece)

D. J. J. van Hinsbergen[1]

Vening Meinesz Research School of Geodynamics, Department of Earth Sciences, Utrecht University, Utrecht, Netherlands

W. J. Zachariasse

Institute for Paleoenvironments and Paleoclimate Utrecht, Department of Earth Sciences, Utrecht University, Utrecht, Netherlands

M. J. R. Wortel and J. E. Meulenkamp[2]

Vening Meinesz Research School of Geodynamics, Department of Earth Sciences, Utrecht University, Utrecht, Netherlands

Received 1 June 2004; revised 20 October 2004; accepted 17 February 2005; published 28 April 2005.

[1] After their emplacement in the course of the late Mesozoic and the Cenozoic, the Hellenic nappes became fragmented during late orogenic extension since the late Eocene. Here we focus on the transition of underthrusting during nappe emplacement to exhumation during late orogenic extension. To this end, we compared previously published data on the structural geological and metamorphic history of the underthrusted parts of the Tripolitza and Ionian nappes, which were exhumed in the Cycladic and South Aegean windows, with newly obtained data on the sedimentary, stratigraphic, and structural development of the part of these nappes in the foreland, in front of the subduction thrust. The results allow the identification of two major events: Event 1 took place around the Eocene-Oligocene transition and marks the onset of underthrusting of the Tripolitza nappe below the Pindos nappe and the Ionian nappe below the Tripolitza nappe, respectively. This led to the uplift and erosion of the Pindos unit and the onset of deposition of the Tripolitza and Ionian flysch in front of the Pindos thrust, together with the formation of mylonites at the base of the metamorphosed portions of the Pindos unit related to the underthrusting of the Tripolitza unit. Event 2 occurred in the latest Oligocene to earliest Miocene and marks the decoupling of the Ionian unit from the underthrusting plate, the accretion of the Tripolitza and Ionian units to the overriding plate, and the onset of late orogenic extension and exhumation in the overriding plate. This led to the formation of the South Aegean and Cycladic core complexes and the subsidence of the Klematia-Paramythia half-graben throughout the early Miocene. **Citation:** van Hinsbergen, D. J. J., W. J. Zachariasse, M. J. R. Wortel, and J. E. Meulenkamp (2005), Underthrusting and exhumation: A comparison between the External Hellenides and the ''hot'' Cycladic and ''cold'' South Aegean core complexes (Greece), *Tectonics*, *24*, TC2011, doi:10.1029/2004TC001692.

1. Introduction

[2] The Aegean nappe stack evolved as a result of African-European convergence in the course of the late Mesozoic and Cenozoic. Previously stacked nappes became subjected to late orogenic extension, starting in northern Greece in the late Eocene [*Gautier et al.*, 1999; *Jolivet et al.*, 2003; *Lips et al.*, 2000], followed by the formation of two windows in central (Cyclades) and southern Greece (Peloponnesos and Crete; Figures 1 and 2), starting around the Oligocene-Miocene transition. [*Avigad et al.*, 1998; *Gautier et al.*, 1993; *Jolivet et al.*, 1996; *Ring et al.*, 2001; *Ring and Reishmann*, 2002; *Thomson et al.*, 1998]. The metamorphic rocks that were exhumed in the Cycladic and South Aegean windows were interpreted to be the underthrusted and metamorphosed equivalents of the non-metamorphosed parts of the Tripolitza and Ionian units exposed in western Greece (Figure 1) [*Jacobshagen*, 1986; *Jolivet et al.*, 2004b; *Kowalczyk and Zügel*, 1997; *Ring et al.*, 2001; *Thiébault*, 1979] (see below). The non-metamorphosed parts of these nappes are well exposed and least fragmented in northwestern Greece, where they deformed in front of the Oligocene Pindos thrust [*IGRS-IFP*, 1966; *Jenkins*, 1972; *Sotiropoulos et al.*, 2003].

[3] In this paper, we aim to reconstruct the transition of underthrusting during nappe stacking to exhumation during late orogenic extension. To this end we compare the geologic histories of the metamorphosed and nonmetamorphosed equivalents of the nappes that are exposed in the External Hellenides and the Cycladic and South Aegean

[1]Now at Department of Geology, University of Leicester, Leicester, UK.
[2]Also at Institute for Paleoenvironments and Paleoclimate Utrecht, Department of Earth Sciences, Utrecht University, Utrecht, Netherlands.

0278-7407/05/2004TC001692$12.00

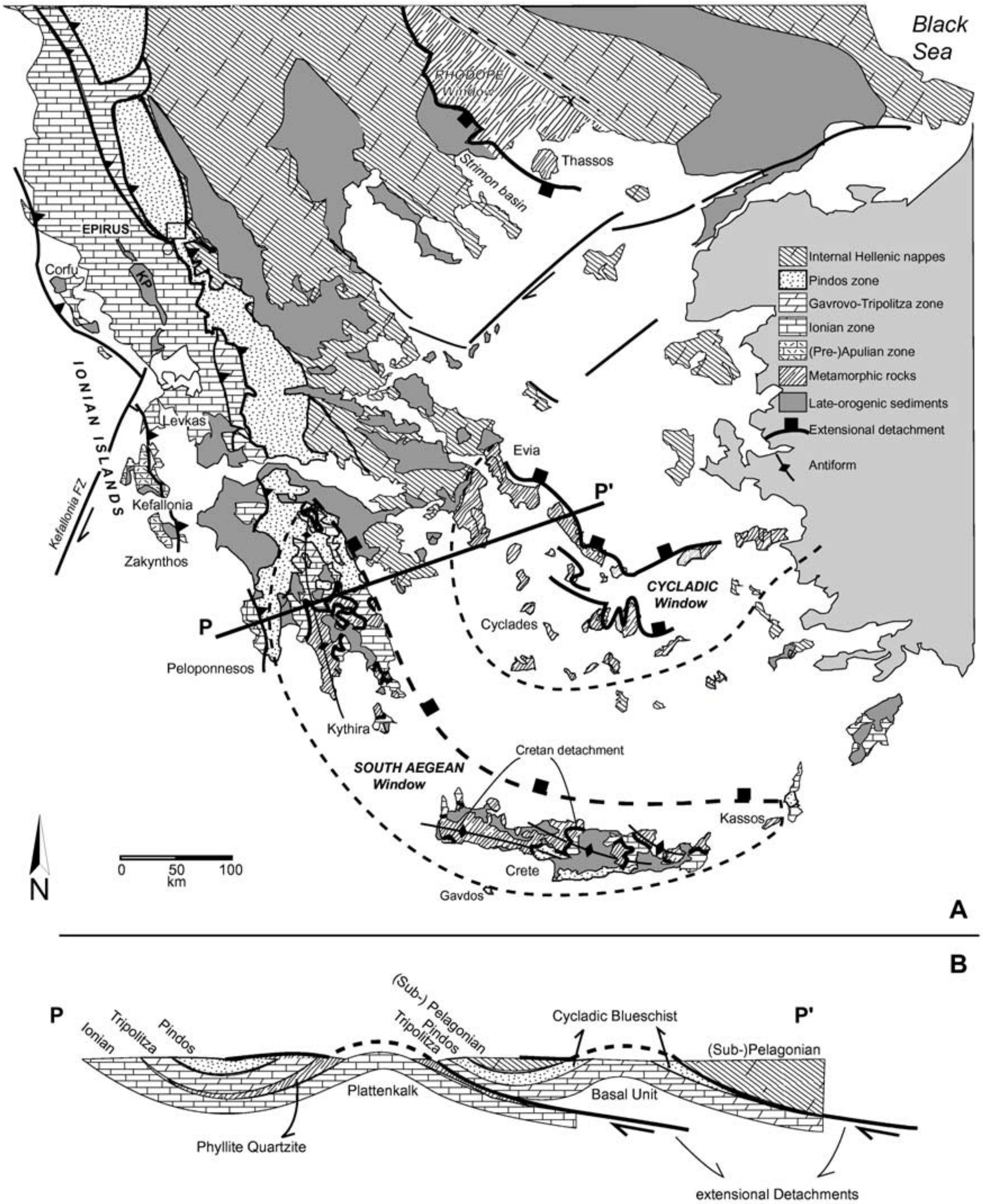

Figure 1. (a) Geologic map of the Aegean region, modified after *Bornovas and Rontogianni-Tsiabaou* [1983], *Dinter* [1998], *Jolivet et al.* [2004b], and *Meco and Aliaj* [2000]. (b) Highly schematic cross section P-P' showing the structure and lithologies of the South Aegean and Cycladic windows. For detailed structural cross sections and correlations, see *Jolivet et al.* [2004a, 2004b].

windows. The data from the metamorphics exposed in the windows are compiled from literature. From the External Hellenides we sampled a number of sedimentary sites and sections in the Oligocene and lower Miocene of the Tripolitza and Ionian units and the structurally underlying pre-Apulian unit (Figure 3) and analyzed the Oligocene and especially early Miocene vertical motion history of the foreland basin based on paleobathymetry estimated [see *Van der Zwaan et al.*, 1990; *van Hinsbergen et al.*, 2005b]. Additionally, paleomagnetic sampling was carried

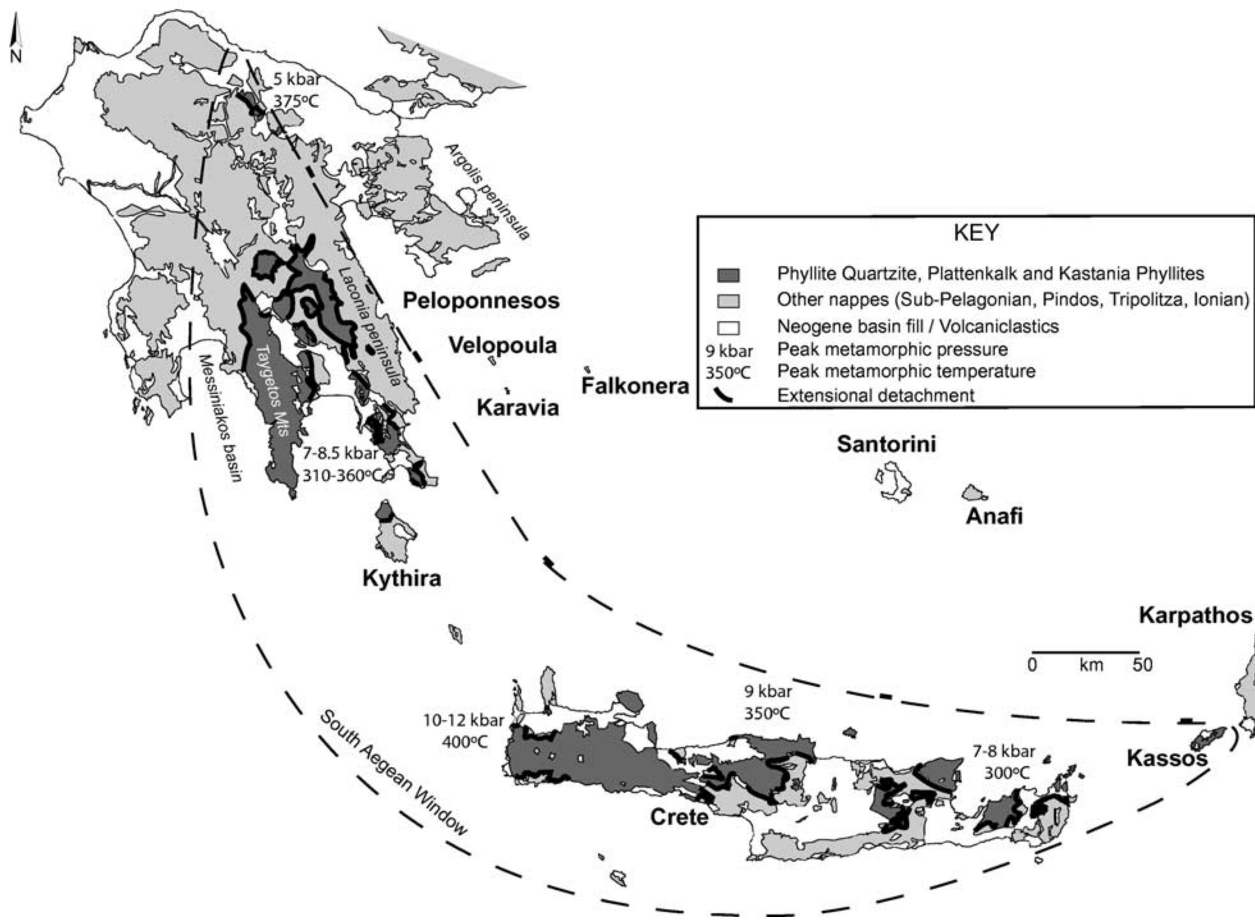

Figure 2. Schematic map, simplified from *Bornovas and Rontogianni-Tsiabaou* [1983], showing the distribution of the South Aegean window. Estimates of peak metamorphic conditions are compiled from *Blümor et al.* [1994], *Brix et al.* [2002], *Jolivet et al.* [1996], *Katagas et al.* [1991], *Theye and Seidel* [1991], *Theye et al.* [1992], *Thomson et al.* [1998, 1999], *Wachmann* [1997], and *Zulauf et al.* [2002].

out to compare the anisotropy of the magnetic susceptibility (AMS) of the Oligocene and lower Miocene of mainland western Greece, since the AMS can be used to determine if stress has been applied to weakly deformed sediments [e.g., *Hrouda*, 1982; *Kissel et al.*, 1986; *Tarling and Hrouda*, 1993]: upon deformation, the maximum axis of the AMS (k_{max}) will gradually align with the direction of maximum extension and perpendicular to the direction of maximum contraction.

2. Geological Setting

[4] Late Mesozoic and Cenozoic convergence between Africa and Europe formed an E-W to ESE-WNW striking, north dipping nappe stack [*Aubouin*, 1957]. The largest part of these nappes was underthrusted below the older nappe stack and metamorphosed, but the most external parts of the nappe remained in their foreland position and did not underthrust. In northwestern Greece, this nonmetamorphosed part of the nappe stack is at present best exposed and least fragmented in northwestern Greece [*IGRS-IFP*, 1966; *Jacobshagen*, 1986], where the nappe-bounding thrusts and associated folds strike NNW-SSE as a result of 50° clockwise, post-early Miocene rotation [*Kissel et al.*, 2003; *van Hinsbergen et al.*, 2005a, and references therein]. The five most external units are from top to bottom the (Sub-) Pelagonian, Pindos, Tripolitza, Ionian and (Pre-) Apulian units (Figures 1 and 3), each with their own distinct lithostratigraphy and separated by thrusts. The (Sub-) Pelagonian unit is the most easterly nappe exposed in western Greece (Figures 1 and 3). The nappe consists of Variscan basement (Pelagonian unit), unconformably overlain by a series of Permian to Jurassic carbonates of varying facies, overthrusted during the Jurassic by an ophiolite complex which is overlain by Cretaceous carbonates and Paleogene flysch [*Baumgartner*, 1985; *Ricou et al.*, 1998]. The Pindos unit comprises Triassic to upper Cretaceous deep-marine carbonates and radiolarites, overlain by up to 4000 m of Paleocene to lower Oligocene flysch [*Richter et al.*, 1978]. The (Gavrovo-) Tripolitza unit structurally underlies the Pindos unit in the east and overthrusted the Ionian unit to the west. It comprises Triassic volcanics overlain by Late Triassic to Eocene platform carbonates [*Jacobshagen*, 1986; *Pe-Piper*, 1982]. The Ionian unit contains (Permo-) Triassic

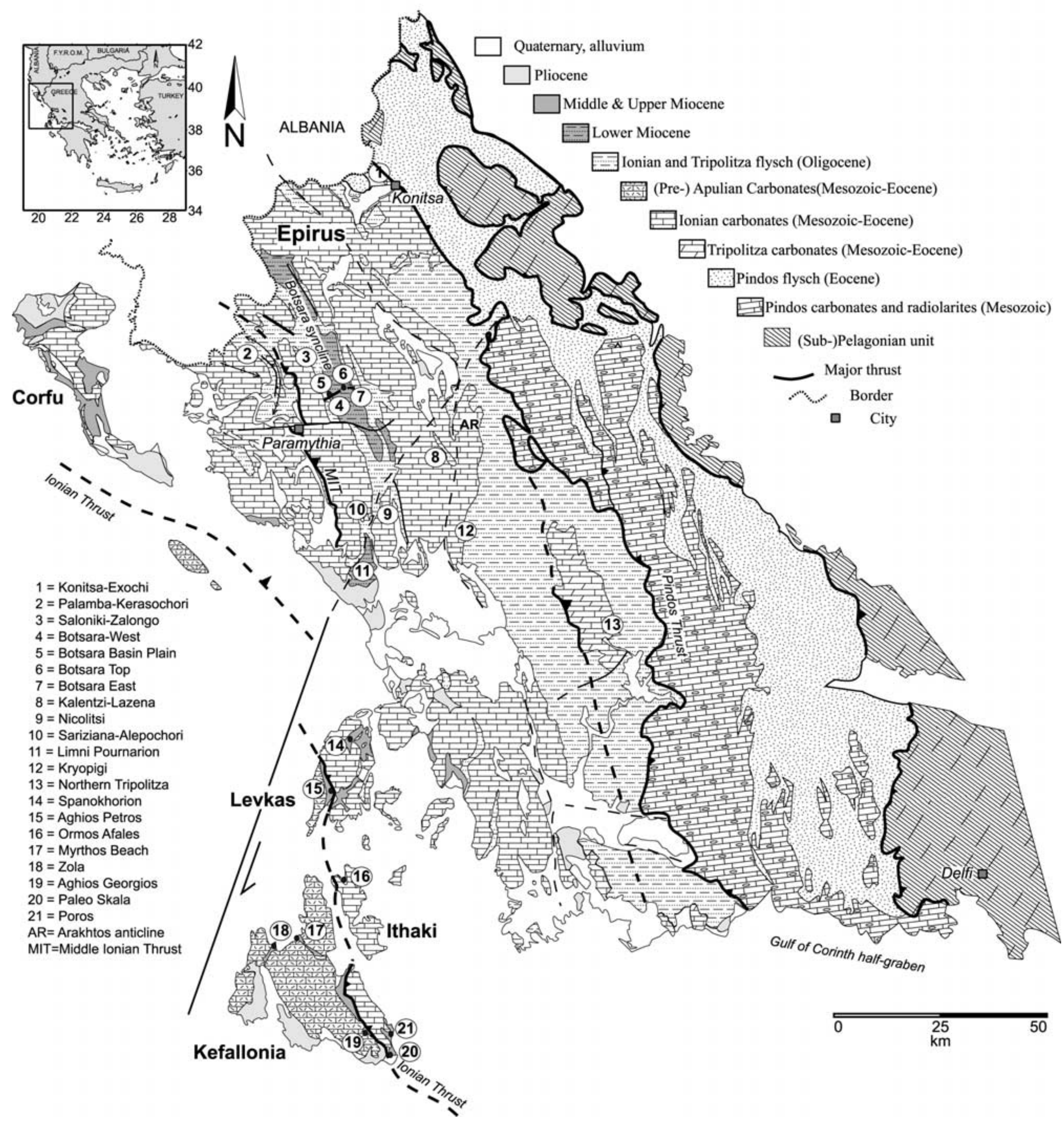

Figure 3. Geologic map of northwestern Greece, modified after *Bornovas and Rontogianni-Tsiabaou* [1983], with sample locations.

gypsum, Triassic to Jurassic platform carbonates and deep-marine well-bedded limestones that structurally underlie the Tripolitza and overthrusted the (Pre-) Apulian unit. In Epirus, internal thrusts subdivide the Ionian unit into the internal, middle and external Ionian units [*IGRS-IFP*, 1966; *Jenkins*, 1972; *Karakitsios*, 1995] (Figure 3). The Tripolitza and Ionian units are overlain by Oligocene deep marine flysch with a thickness of a few hundreds of meters in the external Ionian to more than 5 km in the internal Ionian and Tripolitza units [*IGRS-IFP*, 1966; *Richter et al.*, 1978]. The underthrusting of the Ionian unit below the Tripolitza and of the Tripolitza below the Pindos occurred simultaneously during the Oligocene [*Sotiropoulos et al.*, 2003]. The Pre-Apulian unit on Levkas and Kefallonia exposes continuous Oligocene to lower Miocene deep-marine carbonate successions, with a transition to terrigenous clastics in the course of the late Burdigalian (late early Miocene) to early Langhian (early middle Miocene) (Figure 3) [*De Mulder*, 1975; *IGRS-IFP*, 1966].

[5] Large windows, which expose previously underthrusted and metamorphosed rocks formed in the Hellenic nappes since the late Eocene in northern Greece, and since the early Miocene in central and southern Greece (Figure 1) [*Gautier et al.*, 1999; *Jolivet et al.*, 2003; *Lips et al.*, 2000]. In the following we will focus on the Oligocene and early Miocene geologic development of the Tripolitza and Ionian units, both in the External Hellenides and in the Cycladic and South Aegean windows.

3. Oligocene and Early Miocene History of the External Hellenides

3.1. Oligocene to Lower Miocene Clastics of Western Greece

[6] The nonmetamorphic Tripolitza and Ionian carbonate units in western Greece are overlain by Oligocene deep marine, terrigeneous-clastic flysch deposits with a thickness of a few hundreds of meters in the external Ionian to more than 5 km in the internal Ionian and Tripolitza units [*IGRS-IFP*, 1966; *Richter et al.*, 1978] (Figure 4). Flysch deposition ceased in the internal Ionian and Tripolitza units in the late Oligocene, probably as a result of folding and uplift [*British Petroleum Company* (*BP*), 1971; *IGRS-IFP*, 1966]. The middle Ionian unit was probably also uplifted in the late Oligocene, as suggested by a hiatus between the Oligocene and the lower Miocene [*IGRS-IFP*, 1966]. In the external Ionian unit of Epirus and the Ionian Islands, deposition of terrigeneous clastics was continuous throughout the Oligocene and the early Miocene, with an increase in sedimentation rate and average grain size around the Oligocene-Miocene transition. Approximately 800m of lower Miocene was deposited in the external Ionian unit of Epirus [*Bizon*, 1967; *De Mulder*, 1975; *IGRS-IFP*, 1966]. The Pre-Apulian unit on Levkas and Kefallonia exposes continuous Oligocene to early Miocene deep-marine carbonate successions, with a transition to terrigeneous clastics in the course of the Burdigalian (late early Miocene).

[7] In this paper we focus on the Oligocene to early Miocene development of the middle Ionian unit to identify the nature and causes for the hiatus between the Oligocene and lower Miocene. Different names exist for the early Miocene basin on the middle Ionian unit: *IGRS-IFP* [1966] apply the term Botzara-Ekklisia Basin, and *Avramidis et al.* [2000] use the name Klematia-Paramythia Basin. We apply the name Klematia-Paramythia Basin for the basin such as it existed in the early Miocene, and Botsara-syncline for the structure that evolved after deposition.

[8] Detailed sedimentological analysis of the basin was carried out by *Avramidis and Zelilidis* [2001] and *Avramidis et al.* [2000, 2002], who reported dominantly southwestward sediment transport directions in the Oligocene Ionian flysch, and both southwest and northeastward transport, in combination with longitudinal infill during the early Miocene, indicating early Miocene restriction and elongation of the basin.

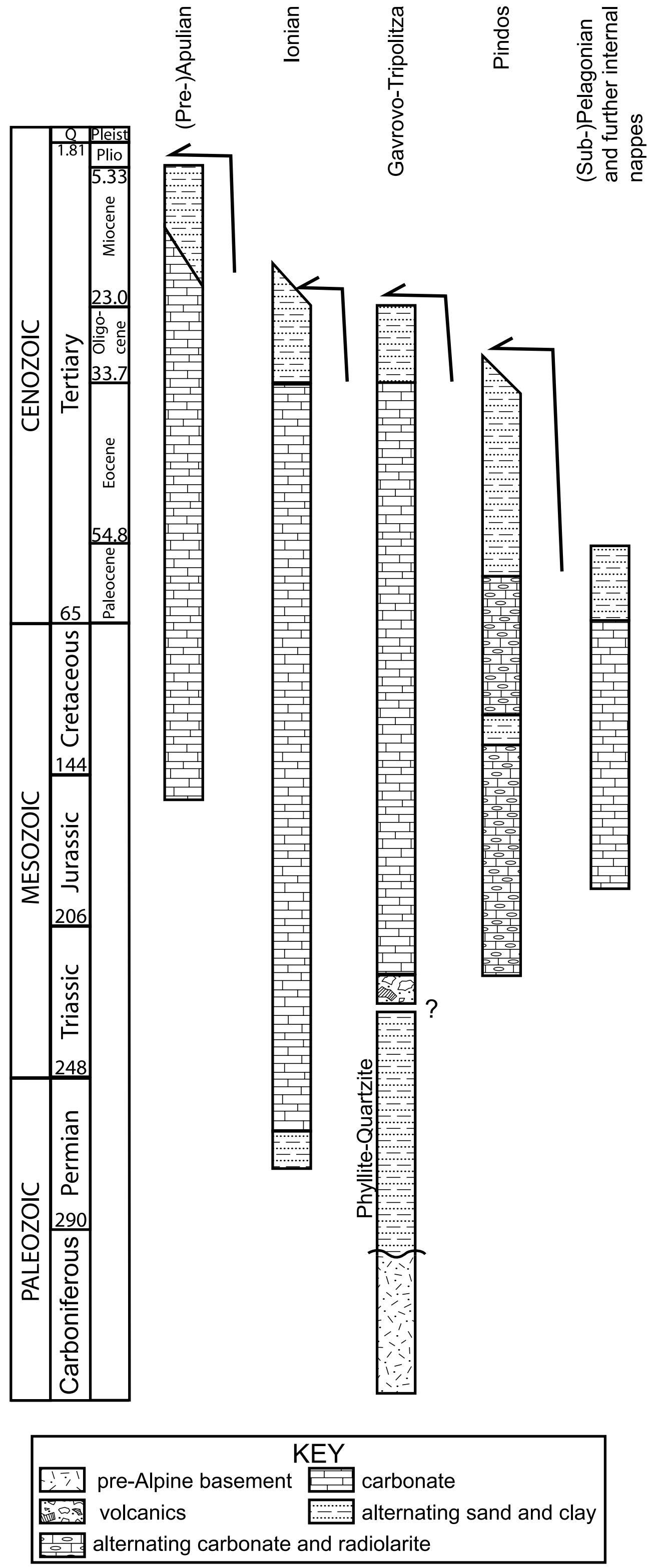

Figure 4. Schematic scheme of the lithostratigraphy of the nappes and timing of nappe emplacement, based on *De Mulder* [1975], *Fleury* [1975], *IGRS-IFP* [1966], *Meulenkamp* [1982], and *Pe-Piper* [1982].

[9] Additionally, we sampled a number of sites and sections in the Oligocene and lower Miocene of the Ionian flysch and the lower Miocene clastics of the Pre-Apulian unit of Epirus, Levkas, Ithaki and Kefallonia for reference.

3.2. Sampling and Ages

[10] The sites from the base of the Ionian flysch (1–3 and 8–13 in Figure 3) correspond with localities that were previously sampled for rotation analysis [*van Hinsbergen et al.*, 2005a]. The base of the Ionian flysch was dated by *IGRS-IFP* [1966], *Peeters et al.* [1998], and *Wilpshaar* [1995] as earliest Oligocene (early Rupelian), on the basis of magnetostratigraphy, dinoflagellate cysts, and planktonic foraminifera, e.g., recovered from outcrops near Saloniki (10) and at the Arakhtos anticline (Figure 3).

[11] Three sections were sampled from the Klematia-Paramythia Basin: Botsara West and East are from the limbs of the syncline and Botsara Top represents the youngest part of the core of the syncline (Figures 2 and 4). The sections contain a lateral component, but the large difference in thickness indicates that the amount of accumulated sediment is much larger in the west than in the east of the basin. The significance of this asymmetry will be discussed below.

[12] The planktonic foraminiferal fauna from Botsara West (3 and 5) and Top (6) and East (7) provide conclusive evidence for an early Oligocene age for the Ionian flysch and an Aquitanian to late Burdigalian age for the entire Klematia-Paramythia Basin fill (Figure 5). This conclusion is in line with the age range reported earlier by *IGRS-IFP* [1966] but is in contrast with the conclusion reached by *Avramidis et al.* [2000] and *Stoykova et al.* [2003], who suggested that the sequence continues into the upper Miocene to lower Pliocene. *Catapsydrax dissimilis* is found up to the 90 m level in the Botsara Top (6), which together with the absence of (prae)orbulinids suggests that the top of the Botsara sequence belongs to unit N6 (the top of which has an age of 17.54 Ma [*Lourens et al.*, 2005]).

[13] The East (7) and West (4) sections are largely time equivalent. The basal parts of both sections contain planktonic foraminiferal faunas indicative of an early Oligocene age (Figure 5): *Globorotalia ampliapertura-increbescens* group, *Globoquadrina venezuelana* and *Catapsydrax dissimilis* in Botsara East (7) and specimens close to *Paragloborotalia opima* s.s., *G. venezuelana* and *C. unicavus* in Botsara West (4). In Botsara East (7), lower Oligocene strata are overlain by strata containing a lower Miocene fauna of planktonic foraminiferal unit N4 characterized by specimens identical or close to *Globorotalia kugleri* and *Globigerinoides primordius/trilobus*, suggesting that the upper Oligocene is missing.

[14] No upper Oligocene faunas were found in Botsara West (4) either. Here, lower Oligocene and lower Miocene (N4) faunas are separated by an unsampled interval of 750 m, which may include (part of) the upper Oligocene. The N4 (Aquitanian) fauna in both sections is followed by faunas characteristic of the N5-N6 unit interval (Figure 5), which in chronostratigraphic terms spans the upper Aquitanian to Burdigalian [*Lourens et al.*, 2005].

[15] *IGRS-IFP* [1966] also reported that the upper Oligocene is missing in the middle Ionian unit. They placed the unconformity around the Aquitanian-Burdigalian boundary, but our data suggest that the hiatus should be placed below the Aquitanian, around the Oligocene-Miocene boundary (Figure 5). The abrupt increase in radiolarians in the lower Miocene of both sections marks a distinct tie line between the eastern and western limb of the syncline. The presence of *Globorotalia dehiscens* in Botsara East (7) and its absence in Botsara West (4) suggest that the top of the East section is younger than the top of the West section. The presence of *Catapsydrax dissimilis* along with the absence of (prae)orbulinids in Botsara Top (6) indicates that the youngest sediments are of Burdigalian age (unit N6). The poor magnetic signal resulted in an overall poor quality magnetostratigraphy and cannot be confidently calibrated to the global polarity timescale (Figure 5).

[16] Two sections were analyzed from Levkas (Figure 3). Spanokhorion (14) was sampled from marly sediments with numerous calcareous mass-transported interbeds overlying the Ionian flysch on East Levkas. The section was previously described and dated by *IGRS-IFP* [1966] *Benda et al.* [1982], *Bizon* [1967], and *De Mulder* [1975] as Burdigalian to early Langhian. The planktonic foraminiferal fauna of Aghios Petros (15) on the Pre-Apulian unit of western Levkas indicates that the section covers the lower middle Miocene to the upper Miocene [*Bizon*, 1967; *IGRS-IFP*, 1966].

[17] The Ionian unit carbonates of the island of Ithaki (Figure 3) are overlain by Oligocene to lower Miocene clays and calcareous turbidites and marly mud flows, are found in the north of the island in the Bay of Afales (16 in Figure 3) [*De Mulder*, 1975; *Hagn et al.*, 1967].

[18] The lower Miocene of the external Ionian flysch of Kefallonia in Poros (21) and Paleo Skala (20), described and dated by *Dremel* [1970] was sampled and analyzed as well. The stratigraphy of the Pre-Apulian unit of Kefallonia consists of a thick Mesozoic to Paleogene series of carbonates, overlain by an Oligocene to lowermost Tortonian series of marls and interbedded turbiditic calcareous sandstones [*BP*, 1971; *Bizon*, 1967; *De Mulder*, 1975]. We sampled three short sections from the lower Miocene (Zola, 18, Aghios Georgios, 19, and Myrthos Beach, 17) of the

Figure 5. Stratigraphic correlations of the sections sampled in the Klematia-Paramythia Basin. Numerical ages are taken from *Berggren et al.* [1995] and *Lourens et al.* [2005]. Circled letters refer to the following fauna: A, presence of *Turborotalia ampliapertura* (top 30.3 Ma); B, presence of *Paragloborotalia opima* s.s. (top 27.1 Ma); C, presence of *Paragloborotalia kugleri* (bottom 23.8 Ma; top 21.5 Ma); D, rapid increase of radiolarians; E, presence of *Globorotalia dehiscens*; F, presence of *Catapsydrax dissimilis* (top 17.54 Ma); G, presence of *Preorbulina sicana* (16.97 Ma). *P. sicana* is absent throughout the sections of the Klematia-Paramythia Basin. Solid (open) circles represent normal (reversed) polarity. Open triangles represent inconclusive polarity.

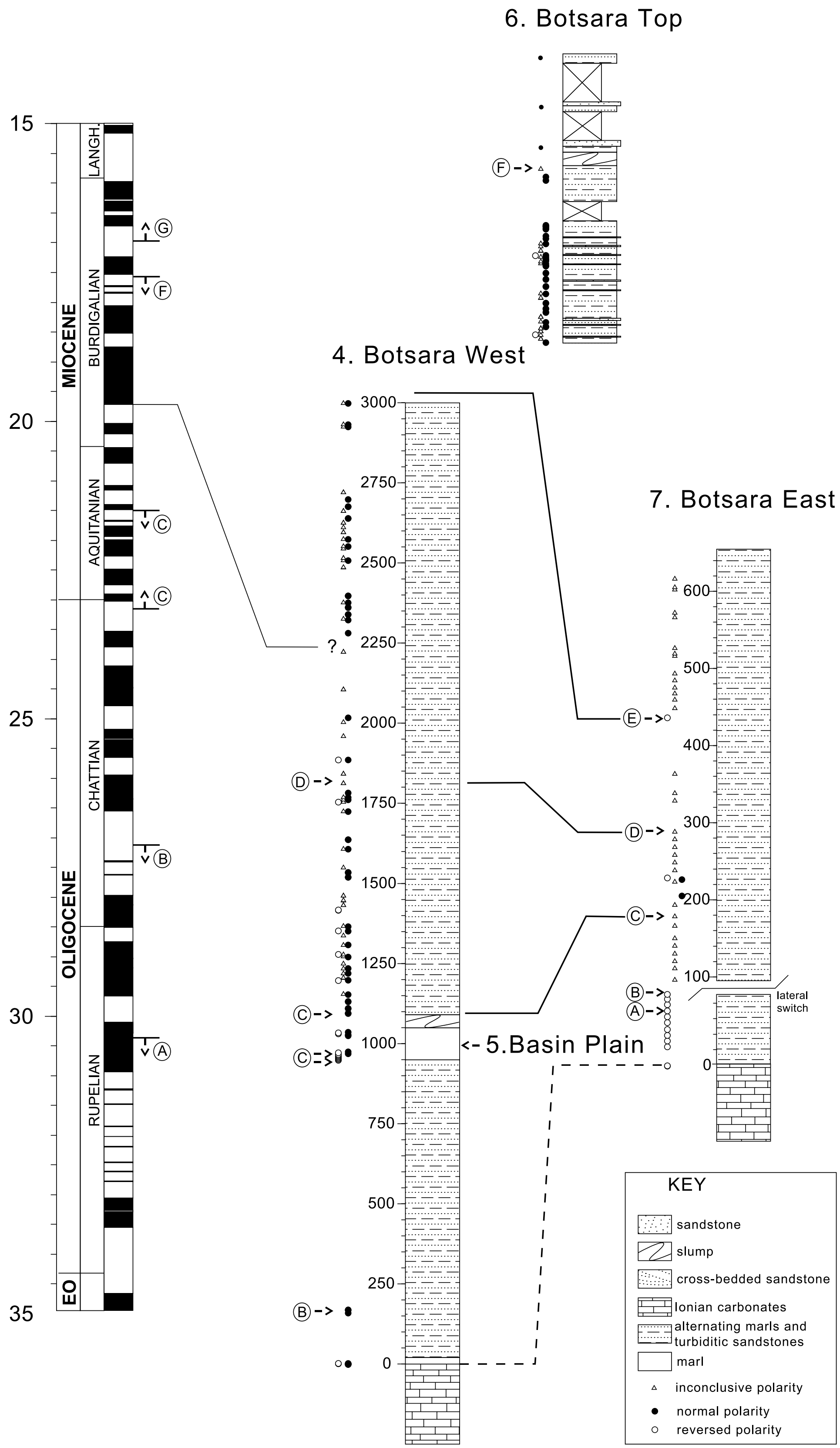
6. Botsara Top
4. Botsara West
7. Botsara East
5.Basin Plain
MIOCENE
OLIGOCENE
EO
LANGH.
BURDIGALIAN
AQUITANIAN
CHATTIAN
RUPELIAN
15
20
25
30
35
lateral switch
KEY
sandstone
slump
cross-bedded sandstone
Ionian carbonates
alternating marls and turbiditic sandstones
marl
inconclusive polarity
normal polarity
reversed polarity

Figure 5

Table 1. Calculated and Estimated Paleobathymetry Values for the Sites and Sections of Epirus, Northwestern Greece[a]

Code	Locality Mainland Greece	Samples (Gr-Code)	n	Depth, m	SD, m	Taxonomic Estimate	Age
1	Konitsa-Exochi	11210-11	1	953	...		early Oligocene
2	Palamba-Kerasochori	11205-09	2	1066	23		early Oligocene
3 and 4	Botsara West and Saloniki Zalongo	11200-04; 12163-65	6	983	97	750–1200	early Oligocene
4 and 5	Botsara West and Basin Plain	12166-240	49	977	95	300–900	early Miocene
6	Botsara Top	12240-275	31	923	72	750–1200	early Miocene
7	Botsara East	12116-26	9	839	105	600–1200	early Oligocene
7	Botsara East	12130-162	26	816	131		early Miocene
8	Kalentzi-Lazena	11220-24	5	1110	96		early Oligocene
9	Nicolitsi	11214-18	5	1034	71		early Oligocene
10	Seriziana-Alepochori	11219	1	1195	...		early Oligocene
11	Limni Pournarion	11225-29	5	1016	89		early Oligocene
12	Kryopigi	11020-26	5	993	56		early Miocene
13	Northern Tripolitza	11230-32	1	1081	...		early Oligocene
14	Spanokhorion (Levkas)	443-471	11	966	71		early Miocene
15	Aghios Petros (Levkas)	12951-12984	28	1096	119	1000+	early–late Miocene
16	Afales Bay (Ithaki)	12469-73	3	718	124	600–1100	early Miocene
17	Myrthos Beach	12452-57	4	913	72	600–1100	early Miocene
18	Zola	12458-67	8	1117	40	>1000	early Miocene
19	Aghios Georgios	12434-41	8	1137	83	600–1100	early Miocene
20	Paleo Skala	KF 1-19	6	978	139	500–900	early Miocene
21	Poros	12442-51	10	986	51	600–1100	early Miocene

[a]Code refers to numbers in Figure 3; n, number of samples averages; SD, standard deviation.

Pre-Apulian unit (Figure 3) to compare their paleobathymetries with the reconstructions for the time equivalent sediments of the Ionian unit.

3.3. Paleobathymetry and Vertical Motions

[19] To estimate the depositional depth of marine sediments, the general relationship between the fraction of planktonic foraminifera with respect to the total foraminiferal population (%P) and depth of *Van der Zwaan et al.* [1990] was used, following sample selection and counting procedures described by *van Hinsbergen et al.* [2005b]. Percentage of P also varies with oxygenation. Generally, with decreasing oxygen levels, the percentage of specific benthic species known as oxygen stress markers with respect to the total population (%S) increased (for more information see *van Hinsbergen et al.* [2005b]. Samples in which %S exceeds 60% were discarded. Generally, %S values were much lower, and no large %S variations were found in the sections. This is logical since deposition in western Greece during the Oligocene and early Miocene occurred in a wide, deep and generally well-ventilated foreland basin [e.g., *Wilpshaar*, 1995]. Some samples contain high fractions of quartz and rock fragments, which here probably result from downslope transport. These samples were discarded.

[20] Depth estimates and their standard deviation are indicated in Table 1. The depth values were checked by means of presence or absence of benthic species indicating specific water depths (for discussion and list, see *van Hinsbergen et al.* [2005b]). The results are included in Table 1, are in line with calculated depth estimates and show that all sampled sites and sections were deep marine (800 to >1000 m) during deposition.

[21] Bathymetry is influenced by sediment supply, eustatic sea level changes, and tectonics. The lack of high-resolution age control made correction for eustatic sea level changes (in the order of tens of meters) impossible. Adding the amount of accumulated sediment to the paleobathymetry at every sample level yields the vertical motion of the base of the section through time (Figure 6), and shows that subsidence must have continued in the Klematia-Paramythia Basin throughout deposition (i.e., at least until ~17 Ma), with much higher subsidence rates in the present SW than NE (Figure 6). No bathymetry changes were reconstructed from the lower Miocene sections of the external Ionian unit and the Pre-Apulian unit (Table 1), but the amount of accumulated sediment here is much less than in the Klematia-Paramythia Basin, in the order of some hundreds of meters [*IGRS-IFP*, 1966].

[22] A sedimentation rate around 50 cm/kyr prevailed during the early Miocene in Botsara West (7). These rates are rather common in basins characterized by turbidite sedimentation. For comparison, the sedimentation rates during the deposition of turbidite sequences of the lower Pliocene of section Corfu Coast on northwestern Corfu [*Linssen*, 1991] or the lower Messinian of section Limni Keri (North) on Zakynthos [*van Hinsbergen*, 2004] are 100 cm/kyr and >125 cm/kyr, respectively.

3.4. Anisotropy of the Magnetic Susceptibility

[23] The anisotropy of the magnetic susceptibility (AMS) can be used to determine if stress has been applied to weakly deformed sediments [e.g., *Hrouda*, 1982; *Kissel et al.*, 1986; *Tarling and Hrouda*, 1993]. If the sediment is undeformed, compaction leads to a magnetic susceptibility that has a random lineation (maximum axis of the AMS, k_{max}), and a bedding-parallel foliation (perpendicular to the minimum axis of the AMS, k_{min}). Upon deformation, the $k_{max\ axis}$ will gradually align with the direction of maximum extension and perpendicular to the direction of maximum contraction. When the amount of contraction exceeds the amount of compaction, the k_{min} axis aligns with the maximum contraction direction.

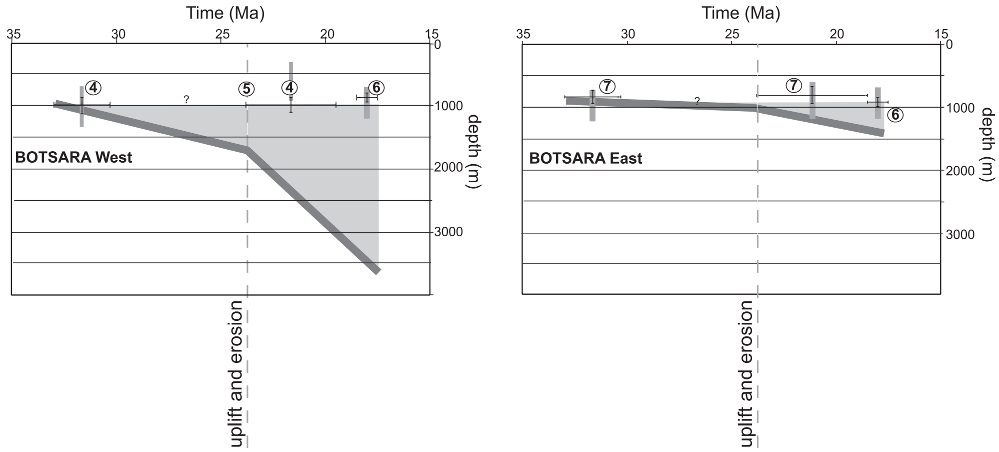

Figure 6. Diagrams of the Klematia-Paramythia Basin, showing the paleobathymetry trends. Adding the amount of accumulated sediment (shaded area) yields the position of the base of the section through time. The amount of subsidence in Botsara West is much higher than time-equivalently in Botsara East.

[24] The AMS has been measured from localities of Oligocene Ionian flysch of the external and middle Ionian units and the lower Miocene of the Klematia-Paramythia Basin (Figures 2 and 5 and Table 2) on a KLY-3 Kappa Bridge. The resulting k_{max} directions obtained from the Oligocene are (sub)parallel to the fold axes and thrust strikes in the vicinity of the locality (Figure 7). The results for the lower Miocene the Klematia-Paramythia Basin, however, show the opposite: the net result of the AMS yields a NE-SW trending k_{max} axis, indicating NE-SW extension (Figure 7).

3.5. Analysis: Oligocene–Early Miocene Geologic History of the External Hellenides

[25] Convergence and underthrusting of the Tripolitza and Ionian units below the Pindos was mainly accommodated by the Pindos and Tripolitza thrusts, respectively, without major internal shortening of the units [e.g., *Sotiropoulos et al.*, 2003]. The Tripolitza unit is not highly folded, probably as a result of the presence of massive platform carbonates, but the well-bedded deep marine Ionian carbonates and overlying flysch were deformed into large antiforms and synforms (Figure 4). The absence of sediments younger than late Oligocene in age in the internal Ionian and Tripolitza units, and the hiatus between the deep-marine lower Oligocene and lower Miocene in the Klematia-Paramythia basin indicate that these folds were at least partly formed around the Oligocene-Miocene transition [see also *IGRS-IFP* [1966]. The emergence and erosion of the Tripolitza and the internal and middle Ionian units led to the deposition of a more proximal clastic facies with higher sedimentation rates in the external Ionian unit [*De Mulder*, 1975; *IGRS-IFP*, 1966]. The external Ionian and the Pre-Apulian units of Levkas and Kefallonia, however, remained deep-marine throughout at least the early Miocene.

[26] After the latest Oligocene or earliest Miocene uplift and erosion of the middle Ionian zone, rapid subsidence formed the Klematia-Paramythia Basin. This subsidence must have been continuous throughout the Aquitanian and Burdigalian to explain the constant depth of 800–1000 m, despite the deposition of 500–2500 m of sediment (Figure 6). Moreover, the amount of subsidence in the southern part of the basin (prior to post-early Miocene rotation) was much higher than in the northern part. The basin floor must therefore have tilted to the south during subsidence and deposition. Such an asymmetry could result from either the formation of a piggyback (thrust-top) basin, or a half-graben. The asymmetry reconstructed from the Klematia-Paramythia basin requires in the piggyback scenario an east directed thrust, cropping out to the present-day northeast of the Klematia-Paramythia basin. The half-graben scenario would require a listric normal fault cropping out to the present-day southwest of the Klematia-Paramythia basin. Neither of these faults is presently observed.

[27] The thickness of the lower Miocene in the external Ionian unit is only approximately 800 m [*IGRS-IFP*, 1966]. Therefore a structure must lie in between the external Ionian zone and the Klematia-Paramythia basin that accommodated the markedly higher subsidence in the Klematia-Paramythia basin. We thus propose that the Middle Ionian Thrust (Figures 3 and 8) that runs parallel to the Klematia-Paramythia basin was a listric normal fault during the early Miocene, and reactivated afterward as a thrust. The half-

Table 2. Results of AMS Analysis for Northwestern Greece, Corrected for Bedding Tilt[a]

Locality	n	Az	dip	dAz	ddip	L
Konitsa-Exochi	7	336.6	6.9	30.2	22.9	1.0122
Aghios Nikolaos–Aghios Pandes	20	128.0	3.3	22.9	6.9	1.0100
Saloniki-Zalongo	52	119.8	8.8	28.9	22.6	1.0066
Klematia-Paramythia basin	262	51.7	8.4	26.8	18.3	1.0066
Nicolitsi 1	9	133.3	14.7	66.3	18.4	1.0024
Nicolitsi 2,4, and 5	30	343.2	44.8	34.7	11.3	1.0068
Kalentzi-Lazena	37	179.4	33.5	56.5	17.8	1.0049
Limni Pournarion	47	179.3	12.8	47.9	23.9	1.0031
Northern Tripolitza	18	188.3	4.1	67.7	16.0	1.0057

[a]See Figure 1 for sample locations; see Table 1 for ages. Definition are as follows: n, number of specimens; Az, mean azimuth; dip, dip of k_{max} axes; dAz and ddip, errors on mean k_{max} axes; L, magnetic lineation (k_{max}/k_{int}).

graben scenario is supported by the AMS results, which for the lower Oligocene sites in Epirus invariably indicate contraction perpendicular to the fold axes, but extension perpendicular to the axis of the Botsara syncline for the lower Miocene of the Klematia-Paramythia Basin (Figure 7).

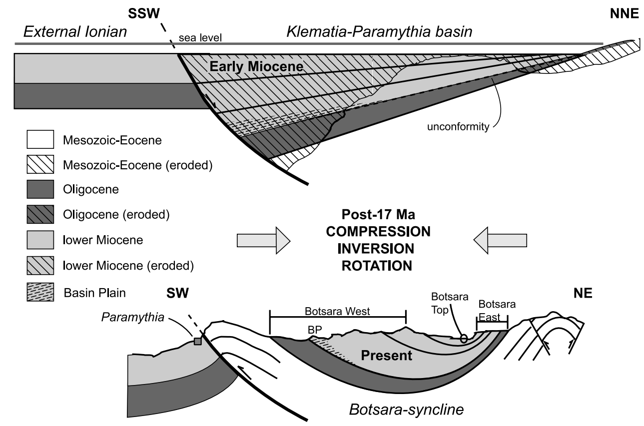

Figure 8. Proposed model for the evolution of the Klematia-Paramythia Basin. After a phase of latest Oligocene uplift and erosion, a north dipping listric normal fault accommodated rapid subsidence in an asymmetric half-graben. The fault must have been continuously active until at least 17 Ma to explain the continuous bathymetry together with the ongoing asymmetric sedimentation. Present-day cross section is modified after *Avramidis et al.* [2002].

[28] In conclusion, our new data show that a phase of uplift and erosion affected the middle Ionian unit between in the late Oligocene or earliest Miocene. This is probably the result of large-scale folding in response to N-S to NNE-SSW contraction that affected the Ionian and Tripolitza units in the late Oligocene [*IGRS-IFP*, 1966; *Sotiropoulos et al.*, 2003]. Our analysis of the Klematia-Paramythia basin shows that this phase of uplift and erosion is followed by approximately N-S to NNE-SSW extension, which rapidly subsided the Klematia-Paramythia half-graben in the earliest Miocene and remained active until after 17 Ma.

4. Oligocene and Early Miocene Geologic History of the Cycladic and South Aegean Windows

4.1. Review of the Metamorphic and Structural Geologic Histories

4.1.1. Cyclades

[29] The Attic-Cycladic metamorphic complex comprises rocks of three different units: an upper unit containing Jurassic and Cretaceous ophiolitic rocks that overthrusted a sequence of Mesozoic carbonates. The upper unit is

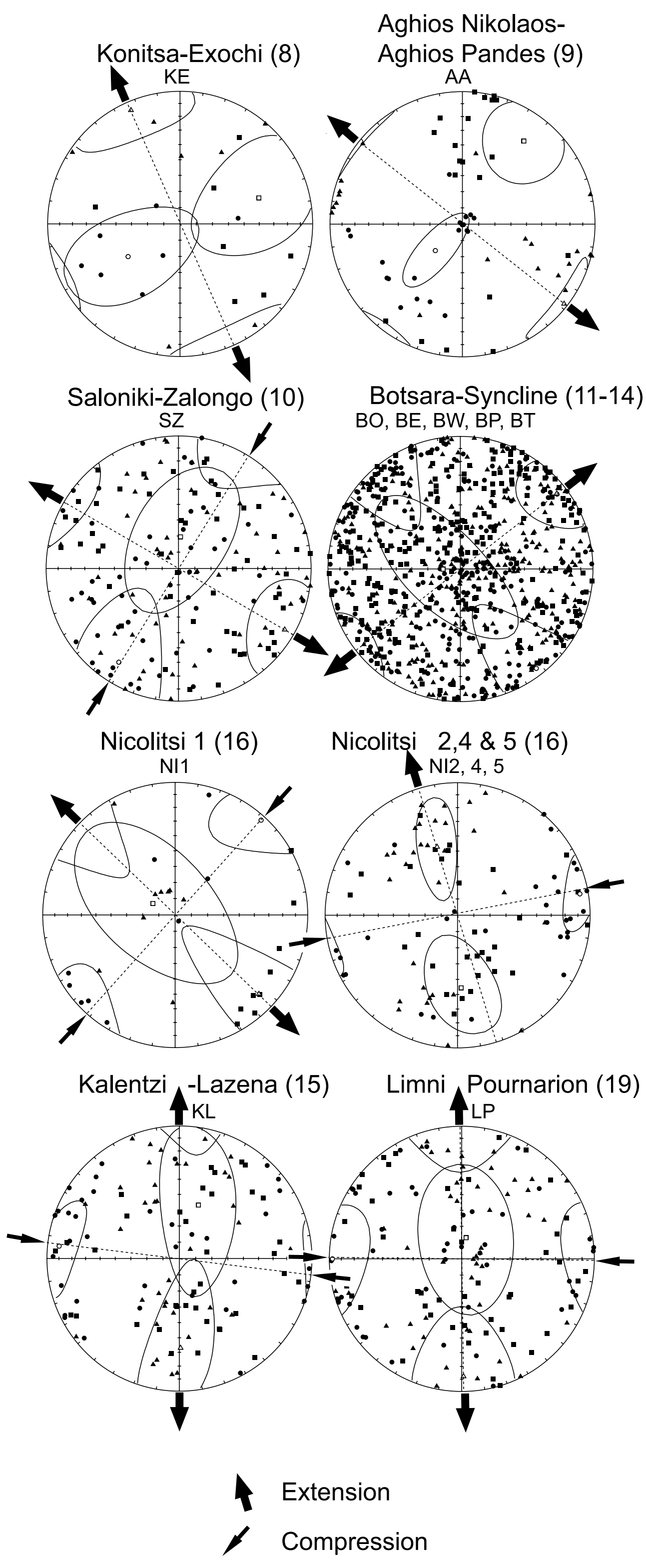

Figure 7. Selection of the results of the AMS analyses. Thick (thin) arrows represent inferred extension (contraction) directions. The contraction and extension directions are in most cases in line with the observed finite deformation pattern in the vicinity of the locality. The only exception is formed by the results of the Botsara syncline, which presently is a NNW-SSE striking syncline, although the AMS results indicate a large influence of ENE-WSW extension. See text for discussion.

separated from the middle unit (Cycladic blueschist) by extensional detachments. The Cycladic blueschist unit consists of metasedimentary and mafic magmatic rocks, overlying a Carboniferous basement [*Ring et al.*, 1999]. The Cycladic blueschist unit was underthrusted by a lower unit (the Basal unit), consisting of platform metacarbonates that reach Eocene sedimentary ages, and Oligocene metaflysch [*Jacobshagen*, 1986; *Jolivet et al.*, 2004b; *Ring et al.*, 2001].

[30] The Basal unit is correlated to the Tripolitza nappe [*Bonneau and Kienast*, 1982; *Ring et al.*, 2001]. The unit was subjected to HP-LT metamorphism during its underthrusting below the Cycladic blueschist unit and peak metamorphic conditions of 8 kbar and 400°C were reached on, e.g., Evia and Samos around 24–21 Ma [*Bröcker and Enders*, 1999; *Ring et al.*, 2001; *Ring and Reishmann*, 2002]. The Cycladic blueschist is believed to be equivalent to the Pindos zone and to the rocks directly underlying the Pelagonian basement on, e.g., the Pelion [*Jacobshagen*, 1986; *Jolivet et al.*, 2004b]. Owing to the large number of islands and their excellent exposure, the metamorphic history of the Cycladic blueschist unit has been subject of many studies. These reveal that peak metamorphic conditions occurred under blueschist to eclogite facies metamorphic conditions of 12–18 kbar and 450°–550°C. Cooling ages obtained by K/Ar, Rb/Sr and $^{40}Ar/^{39}Ar$ dating of minerals that grew during blueschist and eclogite facies metamorphism cluster between 60 and 35–40 Ma (Figure 9). *Bröcker and Enders* [1999] recently suggested that blueschist conditions in the Cycladic blueschist unit already prevailed in the Late Cretaceous, around 70 Ma, on the basis of U-Pb mineral growth ages from Syros; however, *Tomaschek et al.* [2003] showed that these ages do not represent metamorphic ages. Deformation and mineral growth under greenschist facies conditions occurred between approximately 25 and 35 Ma (Figure 9) and is interpreted as the response to underthrusting of the Basal unit below the Cycladic blueschist unit [*Klein-Helmkamp et al.*, 1995]. In the early Miocene, around 22–18 Ma, a retrograde metamorphic overprint occurred, associated with a temperature increase [*Jolivet et al.*, 2003; *Jolivet and Goffé*, 2000]. This is best seen on Naxos, where it led to partial melting [*Buick and Holland*, 1989]. Following this high-temperature overprint, a number of granites intruded the unit, starting on Tinos and Ikaria, and later on Attica, Mykonos, Dilos, Paros, Kos, and Naxos (Figure 9). During the high-temperature overprint, the oldest sediments accumulated in the supradetachment basins, presently exposed on, e.g., Paros and Naxos (Figure 9). The Cycladic blueschist cooled to temperatures below 100°C around 8–6 Ma (Figure 9), which is time-equivalent to the oldest deposits unconformably overlying the Cycladic blueschist unit [*Hejl et al.*, 2002; *van Hinsbergen et al.*, 2004]. Note that the lower to lower middle Miocene sediments on the Cyclades are always in faulted contact with their basement [e.g., *Sánchez-Gómez et al.*, 2002].

[31] The upper unit is found as the hanging wall to the Cycladic extensional detachments and is interpreted as the equivalent of the Pelagonian zone, which is affected by Cretaceous high-temperature metamorphism, associated with the emplacement of ophiolitic rocks. Cretaceous ophiolite emplacement and associated metamorphism is known from southwestern Turkey, Rhodos, Karpathos, Crete [*Hatzipanagiotou*, 1988; *Koepke et al.*, 2002; *Robertson*, 2000], including the Asteroussia nappe [*Seidel et al.*, 1981], Gavdos [*Vincente*, 1970] and some of the Cycladic islands (e.g., Anafi [*Reinecke et al.*, 1982]) and it may be equivalent to the thrusting of the Vardar-Axios zone over the (Sub-) Pelagonian unit (Figure 1).

4.1.2. Southern Aegean

[32] The South Aegean window exposes two HP-LT metamorphic units: the lower Plattenkalk unit and the upper Phyllite Quartzite unit. It is exposed in a curved, lens-shaped window running from the northern Peloponnesos, via Kythira and Crete to the island of Kassos in the southeast (Figure 2). The Plattenkalk unit consists of Paleozoic clastics at the base (Kastania Phyllites), overlain by Mesozoic to Eocene well-bedded carbonates and Oligocene metaflysch and was interpreted as the underthrusted equivalent of the Ionian unit [*Barrier*, 1979; *Bizon and*

Figure 9. Time chart for the Cycladic islands, Evia, and Attica, in which the metamorphic history of the Cycladic blueschist unit is summarized. Note that most ages represent cooling ages, postdating the peak metamorphic conditions of the dated mineral. Reference key is as follows: 1, *Altherr et al.* [1976]; 2, *Altherr et al.* [1979]; 3, *Altherr et al.* [1982]; 4, *Altherr et al.* [1988]; 5, *Allen et al.* [1999]; 6, *Andriessen et al.* [1979]; 7, *Andriessen et al.* [1987]; 8, *Andriessen*, 1991]; 9, *Angelier et al.* [1977]; 10, *Aubourg et al.* [2000]; 11, *Avigad and Garfunkel* [1989]; 12, *Avigad et al.* [1998]; 13, *Baldwin and Lister* [1998]; 14, *Bellon et al.* [1979]; 15, *Besang et al.* [1977]; 16, *Blake et al.* [1981]; 17, *Böger et al.* [1974]; 18, *Böger* [1983]; 19, *Bonneau and Kienast* [1982]; 20, *Bröcker et al.* [1993]; 21, *Bröcker and Franz* [1998]; 22, *Bröcker and Enders* [1999]; 23, *Franz et al.* [1993]; 24, *Fytikas et al.* [1976]; 25, *Fytikas et al.* [1986]; 26, *Gautier et al.* [1993]; 27, *Gautier and Brun* [1994]; 28, *Hejl et al.* [2002]; 29, *Henjes-Kunst and Kreuzer* [1982]; 30, *Henjes-Kunst et al.* [1988]; 31, *Innocenti et al.* [1982]; 32, *Keay et al.* [2001]; 33, *Klein-Helmkamp et al.* [1995]; 34, *Kornprobst et al.* [1979]; 35, *Kreuzer et al.* [1978]; 36, *Lensky et al.* [1997]; 37, *Lister and Raouzaios* [1996]; 38, *Maluski et al.* [1981]; 39, *Matthews and Schliestedt* [1984]; 40, *Meissner* [1976]; 41, *Mpsokos and Pedikatsis* [1984]; 42, *Okrusch et al.* [1978]; 43, *Okrusch and Bröcker* [1990]; 43, *Reinecke* [1986]; 44, *Ring and Layer* [2003]; 45, *Ring et al.* [2003]; 46, *Robert and Cantagrel* [1977]; 47, *Rosenbaum et al.* [2002]; 48, *Sánchez-Gómez et al.* [2002]; 49, *Schliestedt et al.* [1987]; 50, *Schliestedt and Matthews* [1987]; 51, *Sen and Valet* [1986]; 53, *Shaked et al.* [2000]; 54, *Smith et al.* [1996]; 55, *Tomaschek et al.* [2003]; 56, *Trotet et al.* [2001]; 57, *Van Couvering and Miller* [1971]; 58, *Van der Maar and Jansen* [1983]; 59, *van Hinsbergen et al.* [2004]; 60, *Weidmann et al.* [1984]; 61, *Willmann* [1983]; 62, *Wijbrans and McDougall* [1988]; 63, *Wijbrans et al.* [1993]. See color version of this figure at back of this issue.

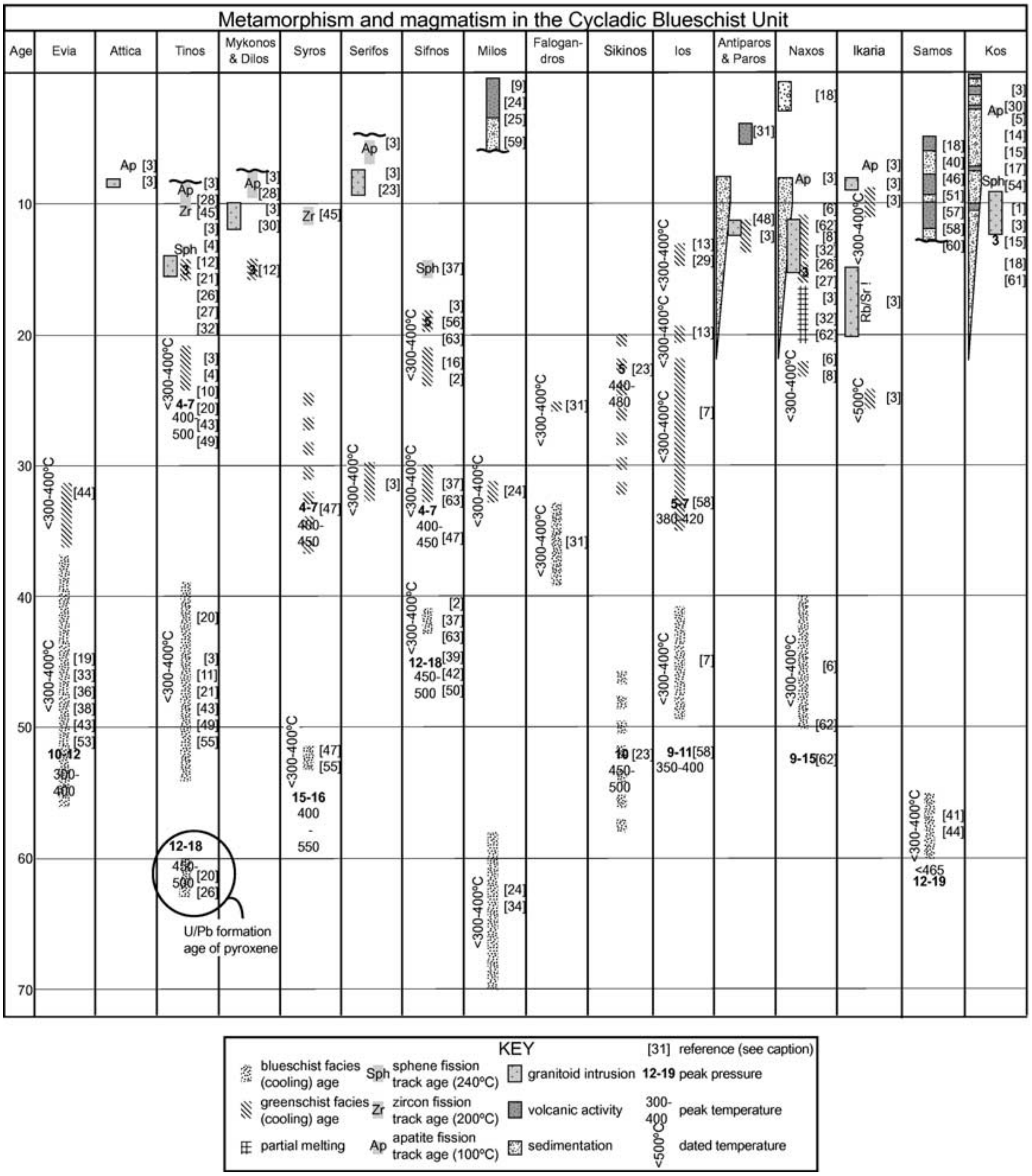

Figure 9

Thiébault, 1974; *Dittmar and Kowalczyk*, 1991; *Kowalczyk and Dittmar*, 1991; *Kowalczyk and Zügel*, 1997; *Thiébault*, 1979]. The overlying Phyllite Quartzite unit constitutes a series of late Carboniferous to Middle Triassic marine phyllites with metavolcanites and quartzites (turbidites) and metaconglomerates (debris flows), unconformably overlying Variscan metamorphosed basement [*Brauer et al.*, 1980; *Finger et al.*, 2002; *Krahl et al.*, 1983, 1986; *Panagos et al.*, 1979; *Seidel et al.*, 1982]. Peak metamorphic conditions in the Phyllite Quartzite unit cluster around 8–12 kbar and 300°–400°C, and $^{40}Ar/^{39}Ar$ cooling ages of 24–20 Ma are interpreted to only shortly postdate peak metamorphic conditions [*Jolivet et al.*, 1996; *Seidel et al.*, 1982; *Stöckhert et al.*, 1999; *Theye and Seidel*, 1991; *Theye et al.*, 1992; *Thomson et al.*, 1998; *Wachmann*, 1997; *Zulauf et al.*, 2002]. *Jolivet et al.* [1996], *Theye and Seidel* [1991], and *Theye et al.* [1992] also reported much higher values of 16 ± 2 kbar from the Phyllite Quartzite unit of western Crete and the 17 ± 4 kbar from the southern Peloponnesos, although these values were doubted by *Brix et al.* [2002]. The Plattenkalk on the Peloponnesos appears to have lower peak metamorphic pressures, with maximum values of 5–8 kbar [*Blümor et al.*, 1994; *Manutsoglu*, 1990].

[33] The comparable timing and conditions of peak metamorphism of the Basal unit on the Cyclades and the Phyllite Quartzite unit on Crete led *Jolivet et al.* [1996] and

Ring et al. [2001] to suggest that these two units were underthrusted together. Moreover, these authors proposed that the exhumation of the Phyllite Quartzite unit occurred along an extensional detachment, reactivating an original subduction thrust between the two. The stratigraphic ages of the Phyllite Quartzite (Paleozoic to Middle Triassic) and the Tripolitza unit (Middle Triassic and younger) suggest, however, that the preexhumation contact was stratigraphic, possibly unconformable, comparable with and equivalent to the contact between the Kastania phyllites and the Plattenkalk described by *Kowalczyk and Dittmar* [1991] (Figure 3).

[34] In summary, the metamorphosed units that are presently exposed in the Cycladic and South Aegean windows most likely represent the underthrusted equivalents of the Ionian, Tripolitza and Pindos units and their original substratum. The Cycladic blueschist, correlated to the Pindos unit, underwent peak metamorphic conditions around 55 to 50 Ma and the Basal unit, Phyllite Quartzite and Plattenkalk units, correlated to the Tripolitza and Ionian zones, underwent peak metamorphic conditions around 24 to 20 Ma.

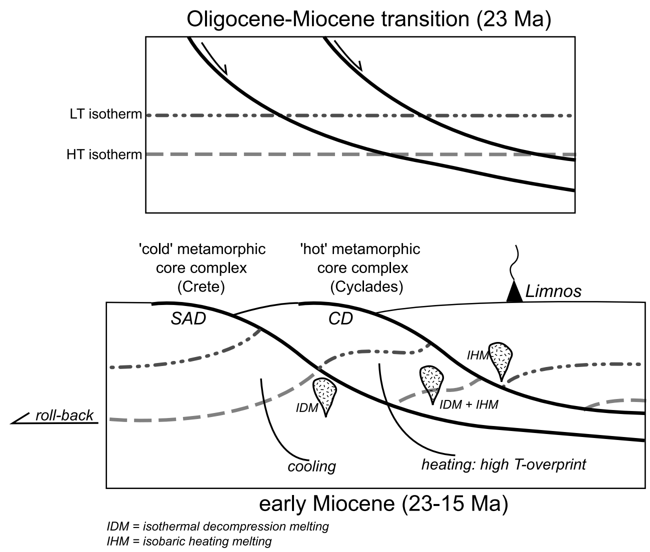

Figure 10. Schematic model of the early Miocene development of Greece along a N-S transect from Crete or the Peloponnesos to the Cyclades (see Figure 1). Exhumation of the "cold" South Aegean core complex leads to a high-temperature event on the Cyclades. Exhumation of the footwall of the South Aegean detachment (SAD) brings high-temperature isotherms in contact with low-temperature isotherms of the hanging wall, leading to a high-temperature event of the hanging wall (i.e., the Basal unit and Cycladic blueschist) and further cooling of the Phyllite Quartzite. The "hot" Cycladic core complex is exhumed along the Cycladic detachment system (CD).

4.2. "Hot" Cycladic Versus "Cold" South Aegean Metamorphic Core Complexes

[35] A metamorphic core complex is primarily characterized by a low-angle extensional detachment, separating a significantly lower metamorphic grade hanging wall from a higher metamorphic grade footwall [e.g., *Lister et al.*, 1984; *Blasband et al.*, 1997]. Additionally, the footwall may have undergone a regional high-temperature, low-pressure (HT-LP) overprint, sometimes associated with granite intrusion.

[36] The first criterion only requires motion along a transcrustal extensional detachment. The HT-LP overprint will only occur, however, in the hanging wall to the extensional detachment: A high-temperature metamorphic overprint is the result of "exhumation" of high-temperature isotherms to bring them in contact with lower temperature material (Figure 10). The granitoids that are frequently described in metamorphic core complexes may result from two processes: the first is partial melting as a result of isothermal decompression of the footwall and the second is isobaric heating of the hanging wall. The formation of a "classical" metamorphic core complex therefore requires two extensional detachments: one below the core complex, which provides the regional high-temperature overprint and isobaric heating-related melting, and one above, exhuming the core complex and leading to decompression melting.

[37] Therefore we introduce a twofold subdivision in metamorphic core complexes (Figure 11). "Cold" metamorphic core complexes are exhumed in the footwall to an extensional detachment. These may have undergone partial melting because of isothermal decompression, but did not experience a high-temperature overprint. "Hot" metamorphic core complexes form the hanging wall to a lower detachment, and the footwall to the upper one, along which the "hot" metamorphic core complex, is exhumed. These core complexes underwent a regional high-temperature overprint, the influence of which decreases upward in the tectonostratigraphy. Moreover, they are intruded by granites generated by decompression in the footwall of the lower detachment. Additionally, partial melting of the hanging wall due to isobaric heating may have occurred. Additionally, isothermal decompression as a result of motion along the upper detachment may have led to decompression melting. The influence of high-temperature metamorphism will be highest at the base of the hanging wall, where advected hot material replaces initially colder lithosphere below the detachment; the intensity of the high-temperature overprint decreases upward, where the lithosphere above the detachment remains cool until it is warmed by conduction [*Buck et al.*, 1988].

[38] We will now apply this concept to the early Miocene history of the south central Aegean region. The early Miocene N-S extension led to the formation of the South Aegean and Cycladic windows. *Jolivet and Goffé* [2000] and *Jolivet et al.* [2003] already noted that the retrograde metamorphic path of the Cycladic blueschist was in places, notably on Naxos, associated with a temperature increase, whereas the rocks in the South Aegean core complex did not. We therefore depict the Cycladic core complex as "hot" and the South Aegean core complex as "cold."

[39] The Cycladic blueschist and Basal unit underwent a retrograde temperature increase, which was most prominent on Naxos. The formation of a "hot" core complex was

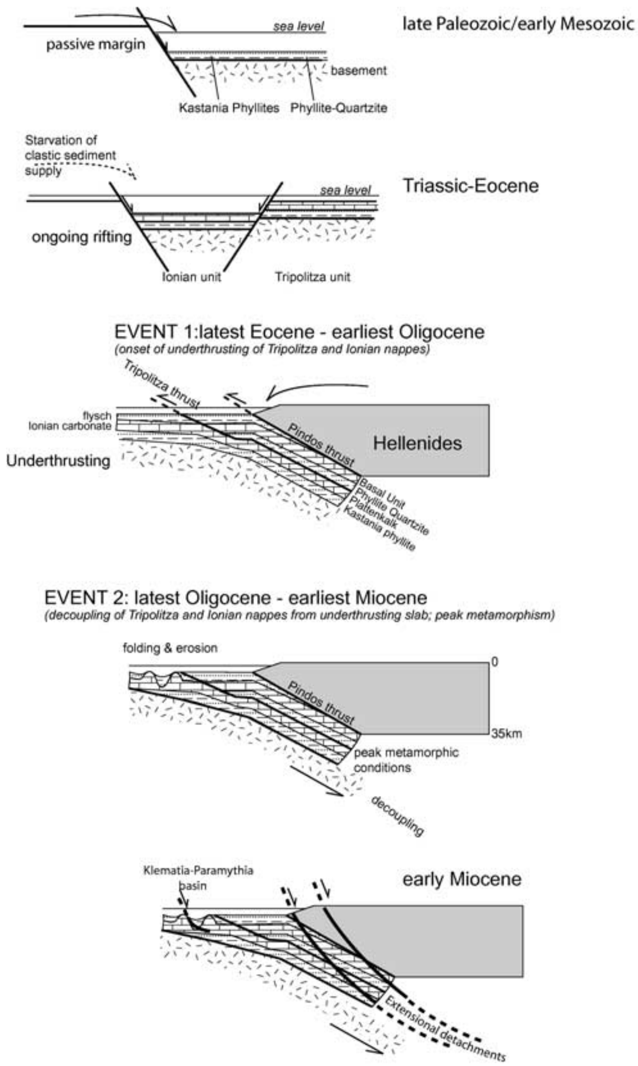

Figure 11. Schematic evolution of the Tripolitza and Ionian units and underlying clastic Kastania Phyllites and Phyllite Quartzite units from their sedimentation during and after the late Paleozoic and Mesozoic rifting to their underthrusting, accretion, and late orogenic extensional exhumation in the early Miocene.

interpreted by *Jolivet et al.* [2003] as the result of southward migration of the volcanic arc. However, the early Miocene volcanic arc lies 200–250 km north of the present-day position of the Cyclades, and it is unlikely that correction for the postmagmatic exhumation of the Cycladic blueschist and Basal unit back into their early Miocene position brings these rocks 200–250 km north underneath the early Miocene volcanic arc.

[40] The simultaneous exhumation of the southern Aegean core complex, however, was not accompanied by such a high-temperature overprint. This was explained by *Jolivet et al.* [2003] and *Thomson et al.* [1999] as a result of continuous underthrusting of cold material below the Phyllite Quartzite and Plattenkalk units during buoyancy-driven exhumation of these units.

[41] Alternatively, we prefer to explain the Cycladic core complex as a "hot" metamorphic core complex. The retrograde temperature increase in the Cycladic area is in this scenario the direct consequence of the simultaneous activity of the South Aegean extensional detachment of Crete and the Peloponnesos. The partial melting on Naxos is associated with temperature increase [*Jolivet et al.*, 2003; *Jolivet and Goffé*, 2000] and is the result of isobaric heating due to of the activity of the South Aegean detachment, and possibly partly of isothermal decompression as a result of motion along the Cycladic detachments. The granites that intruded Naxos probably result from decompression of the footwall of the South Aegean detachment. The South Aegean detachment runs at small angles to the original, probably stratigraphic, contact between the Tripolitza and Phyllite Quartzite units [*Ring et al.*, 2001] and is not underlain by another extensional detachment. Consequently, the South Aegean core complex is "cold" (Figure 10).

4.3. On the Shape of the "Cold" South Aegean Core Complex

[42] The South Aegean core complex has a curved lens-shape, running from the northern Peloponnesos, over Crete to Kassos (Figure 2). The majority of exhumation in the core complex occurred prior to 15 Ma [*Thomson et al.*, 1998]. The middle to late Miocene $\sim 50°$ clockwise rotation of western Greece did most likely not affect Crete, deduced from the $\sim 50°$ angle between the stretching lineations in the Phyllite Quartzite of the Peloponnesos and Crete [*Jolivet et al.*, 2003], explaining the modern curved shape of the core complex. The detachment was thus characterized by a low-angle north dipping orientation with top-to-the-north shear. The lens-shape of the South Aegean core complex (Figure 2) indicates that the maximum amount of extension was accommodated in the center window, i.e., on present-day western Crete and the southern Peloponnesos, decreasing to the north and east. This is in line with the decreasing peak metamorphic conditions of the Phyllite-Quartzite unit from the center of the South Aegean core complex to its northern and eastern ends (Figure 2). *Blümor et al.* [1994] estimated peak metamorphic conditions of 7–8.5 kbar and 310°–360°C from the Kastania Phyllites, underlying the Plattenkalk on the Peloponnesos. If the estimates of the peak metamorphic conditions in the Phyllite Quartzite unit on the southern Peloponnesos and western Crete of 16–17 kbar of *Jolivet et al.* [1996], *Theye and Seidel* [1991], and *Theye et al.* [1992] are correct, these imply that approximately half of the exhumation of the Phyllite Quartzite unit occurred prior to or during the underthrusting by the Ionian/Plattenkalk. We take the value estimated by *Blümor et al.* [1994] as the maximum depth of exhumation in the South Aegean core complex on the southern Peloponnesos. Any older exhumation of the Phyllite Quartzite unit must have been synorogenic (i.e., occurring during underthrusting of the Plattenkalk below the Phyllite Quartzite), which was previously proposed by *Jolivet et al.* [2003] and *Thomson et al.* [1999].

[43] *Ring et al.* [2001] suggested that the Cretan detachment reworked the original contact between the Phyllite

Quartzite and the Tripolitza, which we above argued to have been an unconformity. In many places on Crete, the Tripolitza unit directly overlies the Plattenkalk, separated by the extensional detachment, and the Phyllite Quartzite unit is missing. Therefore the extensional detachment in places crosscuts the entire Phyllite Quartzite unit. *Ring et al.* [2001] estimated that the Cretan detachment accommodated more than 100 km of extension along an on average 10°–15° dipping detachment, assuming that the Phyllite Quartzite unit was originally in direct contact with the Basal unit (Tripolitza) of the Cyclades. Here, we estimate the amount of extension on the basis of the dimension and peak metamorphic conditions of the South Aegean core complex. On the southern Peloponnesos, the width, peak metamorphic conditions and postexhumation deformation history is well known.

[44] On the southwestern Peloponnesos, the Tripolitza unit is overthrust by the Pindos unit. Further to the east, the exhumed Tripolitza unit reappears in the core complex, underlain by the Phyllite Quartzite, Plattenkalk and Kastania Phyllite units. The latter underwent a peak pressure of 7–8.5 kbar [*Blümor et al.*, 1994], corresponding to 25 to 30 km of depth, assuming an average crustal density of 2850 kg/m^3 (following *McKenzie* [1978]). If we assume the center of the exposed Pindos unit on the southern Peloponnesos to be the most westerly part of the extensional detachment, the total horizontal displacement associated with the exhumation of the Kastania Phyllites is approximately 40 km.

[45] Comparable to the situation on Crete, the detachment fault on the southern Peloponnesos is folded and later crosscut by normal faults. In the studied transect between the Kastania Phyllites and the external Pindos unit, a half-graben developed since the late Pliocene (the Messiniakos basin). A seismic profile of *Papanikolaou et al.* [1988] revealed a high-angle (~60°), west dipping normal fault with a net displacement of approximately 3 km. The horizontal component of late Pliocene extension is therefore only about 1 km. The Taygetos unit (Figure 2) exposes a large, asymmetric antiform with a subvertical western and shallow dipping eastern limb [*Doutsos et al.*, 2000], resulting from approximately ~3–5 km of shortening. Therefore the modern 40 km distance between the Kastania Phyllites and the external edge of the core complex was probably little more, in the order of 45 km, prior to postexhumation deformation. Exhumation from a depth of 25 km with ~45 km of horizontal extension implies an original average orientation of the detachment of ~30°. Because the peak pressure estimates do not dramatically change parallel to the stretching direction to the northeast, the detachment probably had a decreasing dip with increasing depth. The eastern coast of the Laconia Peninsula (Figure 2) still exposes the Phyllite Quartzite unit, whereas the Argolis Peninsula entirely belongs to the (Sub-) Pelagonian unit and therefore most likely belongs to the hanging wall of the extensional detachment. To the southeast of the Argolis peninsula, the islets of Velopoula, Falkonera and Karavia expose ultramafic rocks, carbonates and metamorphics associated with the (Sub-) Pelagonian and higher units, as do the islands of Santorini and Anafi, giving a rough indication of the shape and maximum size of the South Aegean core complex. The total amount of horizontal extension on the southern Peloponnesos is thus ~100 km, which is in line with the estimate of *Ring et al.* [2001].

[46] In summary, the South Aegean core complex formed between 24–20 Ma and at least 15 Ma, running from the northern Peloponnesos to Kassos (Figure 2). Prior to the middle to late Miocene rotation phase of western Greece and the southward translation of Crete, the core complex was ~E-W trending, with a lens-shape resulting from the highest displacement of approximately 100 km in the central part, presently exposed on western Crete and the southern Peloponnesos.

5. Time Relationships Between the External Hellenides and the Cycladic and South Aegean Core Complexes

[47] The detailed Oligocene and early Miocene tectonic history that was determined from both the underthrusted and metamorphosed part in the South Aegean core complex and the nonmetamorphosed foreland-basin parts of the Tripolitza and Ionian units in the External Hellenides shows remarkable time relationships, which allows the identification of two marked events.

5.1. Event 1: Eocene-Oligocene Transition

[48] The oldest cooling ages from greenschist facies mylonites associated with underthrusting of the Tripolitza-Basal unit underneath the Cycladic blueschist are 35–30 Myr old. This is comparable in age to the rapid transition from carbonate to terrigeneous clastic sedimentation in the entire Tripolitza and Ionian units [*IGRS-IFP*, 1966; *Peeters et al.*, 1998; *Wilpshaar*, 1995] and the onset of the formation of the Tripolitza-thrust in western Greece [*Sotiropoulos et al.*, 2003]. We therefore interpret Event 1 as the onset of underthrusting of the Tripolitza-Basal unit-Phyllite Quartzite underneath the Pindos-Cycladic blueschist unit and Ionian unit below the Tripolitza-Basal unit-Phyllite Quartzite.

5.2. Event 2: Oligocene-Miocene Transition

[49] Peak metamorphic conditions in the underthrusted parts of the Basal unit/Tripolitza and underlying Phyllite Quartzite units of 24–20 Ma are comparable in age with the end of flysch deposition on and the folding of the Tripolitza and internal and middle Ionian units. The folding and deformation is followed by the onset of exhumation of the Cycladic and South Aegean core complexes, which starts approximately simultaneously in the earliest Miocene and occurs throughout the early Miocene contemporaneously with the formation of the Klematia-Paramythia half-graben in the External Hellenides of western Greece. Moreover, the bounding normal faults of both the Klematia-Paramythia basin and the South Aegean and Cycladic core complexes are characterized by top-to-the-north motion, although the Klematia-Paramythia basin accommodates only a few

kilometers of extension, as opposed to 100 km in the widest part of the South Aegean core complex. Event 2 therefore marks the transition of underthrusting and N-S contraction to exhumation and N-S extension, and an outward shift of the main subduction thrust. These time relationships allow the detailed reconstruction of the transition of underthrusting during nappe stacking to exhumation during late orogenic extension.

6. Reconstruction of the Transition From Underthrusting to Exhumation

[50] Before we focus on the Oligocene to early Miocene history of underthrusting and exhumation of the Tripolitza and Ionian units, we will first summarize the paleoenvironmental setting prior to the Oligocene. In the late Paleozoic, marine clays intercalating with probably mass-transported sandstones and conglomerates (Phyllite Quartzite and Kastania Phyllites [*Dittmar and Kowalczyk*, 1991; *Kowalczyk and Dittmar*, 1991; *Krahl et al.*, 1983, 1986]) were deposited on Variscan or older metamorphosed basement [*Finger et al.*, 2002; *Krahl et al.*, 1986; *Seidel et al.*, 1982]. We therefore suggest that these units represent passive margin deposits.

[51] Event 1, i.e., the onset of underthrusting of the Tripolitza and Ionian units below the Pindos and Tripolitza unit, respectively, is contemporaneous with the uplift and erosion of the Pindos unit [*Richter et al.*, 1978]. The peak metamorphic pressures of approximately 10 kbar in the Basal unit (Tripolitza) and in those times underlying Phyllite Quartzite unit [*Ring et al.*, 2001] indicates that the Pindos thrust must have been continuous to a depth of at least ~35 km.

[52] The earliest major folding and shortening phase of the Ionian unit (Event 2) took place around the Oligocene-Miocene boundary and coincides with the timing of peak metamorphism in the underthrusted parts, indicating that further underthrusting of the Tripolitza and Ionian units along the Pindos thrust was obstructed, leading to internal shortening and folding of the foreland basin. We propose that the folding of the Ionian unit relates and the end of further increase in peak metamorphic conditions in the underthrusted parts of the nappes relates to the decoupling of the Ionian unit from the underthrusting plate. The Tripolitza–Phyllite Quartzite unit must already have been decoupled in the early Oligocene, since it was underthrusted by the Ionian unit since this time. The latest Oligocene-earliest Miocene decoupling of the Ionian unit from the underthrusting plate was followed by rapid exhumation and extension of the overlying crust, as a result of the gravitational response to roll-back and buoyancy forces, or upward extrusion [*Doutsos et al.*, 2000; *Jolivet et al.*, 1994, 2003; *Lips*, 1998; *Ring and Layer*, 2003; *Ring et al.*, 2001; *Thomson et al.*, 1999; *Xypolias et al.*, 2003; *Xypolias and Koukouvelas*, 2001]. We therefore conclude that Event 2 corresponds to the decoupling around the Oligocene-Miocene transition of the entire nappes from the underthrusting plate and their accretion to the overriding plate from the foreland part at least 35 km of depth, followed by the extension and exhumation of the units in the overriding plate.

7. Conclusions

[53] In this paper, we aim to reconstruct the transition of underthrusting during nappe stacking to exhumation during late orogenic extension. To this end we compare the geologic histories of the metamorphosed and nonmetamorphosed equivalents of the nappes that are exposed in the External Hellenides and the Cycladic and South Aegean core complexes.

[54] Detailed investigation of the Klematia-Paramythia basin in the middle Ionian unit of the External Hellenides shows, that following a phase of late Oligocene uplift and erosion as a result of shortening, early Miocene extension created the Klematia-Paramythia half-graben in response to approximately N-S extension. This new information provides accurate time constraints on the transition of contraction to extension around the Oligocene-Miocene transition in the External Hellenides. Comparison of the geological evolution of the Ionian and Tripolitza nappes in the External Hellenides with their underthrusted parts in the Cycladic and South Aegean core complexes allowed the identification of two large-scale events: Event 1 marks the onset of underthrusting of the Tripolitza and Ionian units below the Pindos and Tripolitza units, respectively around the Eocene-Oligocene transition. Around the Oligocene-Miocene transition, Event 2 marks peak metamorphic conditions in the underthrusted portions of the Tripolitza and Ionian nappes, contemporaneous with the uplift and folding of the parts of the nappes in the forelands, followed by the onset of extension and formation of the Klematia-Paramythia basin and the Cycladic and South Aegean core complexes. Event 2 therefore marks the decoupling of the Ionian nappe from the underthrusting plate and their accretion to the overriding plate, followed by the onset of late orogenic extension and exhumation of the Tripolitza and Ionian nappes in the overriding plate.

[55] The exhumation of the underthrusted portions occurred in the "hot" Cycladic and "cold" South Aegean core complexes. A hot core complex is both underlain and overlain by an extensional detachment: The upper one leads to exhumation of the core complex; the lower one provides a regional high-temperature overprint by placing hot material underneath the core complex. A cold core complex is only bounded by one extensional detachment above it, leading to exhumation without a high-temperature overprint. The formation of the South Aegean core complex, exhuming along the South Aegean or Cretan detachment that dips below the Cycladic core complex, therefore provides the high-temperature overprint of the Cycladic core complex.

[56] **Acknowledgments.** This paper benefited significantly from thorough reviews of Uwe Ring and Laurent Jolivet. Pavlos Avramidis (Sedimentological Laboratory, University of Patras, Greece) is kindly thanked for the excursion days in the Klematia-Paramythia Basin and the stimulating discussions. Reinoud Vissers, and Cor Langereis are acknowledged for the critical review of earlier versions of the manuscript. Mark-Jan Sier, Suzanne Bijl, Ioannis Vakalas, Georgios Ananiadis, and Aris

Mantzios are thanked for their assistance during the sampling campaigns of 2002 and 2003. Paul Meijer is acknowledged for the discussion on the development of the Klematia-Paramythia Basin. Marianne Leewis carried out the paleomagnetic measurements on the samples of the Klematia-Paramythia Basin. Gerrit van "t Veld and Geert Ittman are thanked for the preparation of the samples that were used for foraminiferal analysis. The Institute of Geology and Mineral Exploration of Greece (IGME) is thanked for providing the necessary working permits. This project was conducted under the research program of the Vening Meinesz Research School of Geodynamics (VMSG). This is an ISES publication.

References

Allen, S. R., E. Stadlbauer, and J. Keller (1999), Stratigraphy of the Kos Plateau Tuff: Product of a major Quaternary explosive rhyolitic eruption in the eastern Aegean, Greece, *Int. J. Earth Sci.*, *88*, 132–156.

Altherr, R., J. Keller, and K. Kott (1976), Der jungtertiäre Monzonit von Kos und sein Kontakthof (Ägäis, Griechenland), *Bull. Soc. Geol. Fr.*, *18*, 403–412.

Altherr, R., M. Schliestedt, M. Okrusch, E. Seidel, H. Kreuzer, W. Harre, H. Lenz, I. Wendt, and G. A. Wagner (1979), Geochronology of high-pressure rocks of Sifnos (Cyclades, Greece), *Contrib. Mineral. Petrol*, *70*, 245–255.

Altherr, R., H. Kreuzer, I. Wendt, H. Lenz, G. A. Wagner, J. Keller, W. Harre, and A. Hohndorf (1982), A late Oligocene/early Miocene high temperature belt in the Attica Cycladic crystalline complex (SE Pelagonian, Greece), *Geol. Jahrb., Reihe E*, *23*, 97–164.

Altherr, R., F. Henjes-Kunst, A. Matthews, H. Friedrichsen, and B. T. Hansen (1988), O-Sr istotopic variations in Miocene granitoids from the Aegean: Evidence for an origin by combined assimilation and fractional crystallisation, *Contrib. Mineral. Petrol.*, *100*, 528–541.

Andriessen, P. A. M. (1991), K-Ar and Rb-Sr age determinations on micas of impure marbles of Naxos, Greece: The influence of metamorphic fluids and lithology on the blocking temperature, *Schweiz. Mineral. Petrogr. Mitt.*, *71*, 89–99.

Andriessen, P. A. M., N. A. I. M. Boelrijk, E. H. Hebeda, H. N. A. Priem, E. A. T. Verdurmen, and R. H. Verschure (1979), Dating the events of metamorphism and granitic magmatism in the Alpine Orogen of Naxos (Cyclades, Greece), *Contrib. Mineral. Petrol*, *69*, 215–225.

Andriessen, P. A. M., G. Banga, and E. H. Hebeda (1987), Isotopic age study of pre-Alpine rocks in the basal units on Naxos, Sikinos and Ios, Greek Cyclades, *Geol. Mijnbouw*, *66*.

Angelier, J., J.-M. Cantagrel, and J.-C. Vilminot 1977, Néotectonique cassante et volcanisme plio-quaternaire dans l'arc égéen interne: L'île de Milos (Grèce), *Bull. Soc. Geol. Fr.*, *19*, 119–124.

Aubouin, J. (1957), Essai de corrélation stratigraphique de la Grèce occidentale, *Bull. Soc. Geol. Fr.*, *7*, 281–304.

Aubourg, C., R. Hebert, L. Jolivet, and G. Cartayrade (2000), The magnetic fabric of metasediments in a detachment shear zone: the example of Tinos island (Greece), *Tectonophysics*, *321*, 219–236.

Avigad, D., and Z. Garfunkel (1989), Low-angle faults above and below a blueschist belt—Tinos island, Cyclades, Greece, *Terra Nova*, *4*, 182–187.

Avigad, D., G. Baer, and A. Heimann (1998), Block rotations and continental extension in the central Aegean Sea: Palaeomagnetic and structural evidence from Tinos and Mykonos (Cyclades, Greece), *Earth Planet. Sci. Lett.*, *157*, 23–40.

Avramidis, P., and A. Zelilidis (2001), The nature of deep-marine sedimentation and palaeocurrent trends as evidence of Pindos foreland basin fill conditions, *Episodes*, *24*, 252–256.

Avramidis, P., A. Zelilidis, and N. Kontopoulos (2000), Thrust dissection control of deep-water clastic dispersal patterns in the Klematia-Paramythia foreland basin, western Greece, *Geol. Mag.*, *137*, 667–685.

Avramidis, P., A. Zelilidis, I. Vakalas, and N. Kontopoulos (2002), Interactions between tectonic activity and eustatic sea-level changes in the Pindos and Mesohellenic basins, NW Greece, *J. Pet. Geol.*, *25*, 53–82.

Baldwin, S. L., and G. S. Lister (1998), Thermochronology of the South Cyclades Shear Zone, Ios, Greece: Effects of ductile shear in the argon partial retention zone, *J. Geophys. Res.*, *103*, 7315–7336.

Barrier, É. (1979), Précisions sur lédifice des napes helléniques dans lárc égéen oriental: Le jalon de Kassos (Dodécanèse, Grèce), *C. R. Acad. Sci., Ser. D*, *289*, 453–456.

Baumgartner, P. O. (1985), *Jurassic Sedimentary Evolution and Nappe Emplacement in the Argolis Peninsula (Peloponnesus, Greece)*, Birkhäuser Boston, Cambridge, Mass.

Bellon, H., J. J. Jarrige, and D. Sorel (1979), Les activités magmatique égéennes de l'Oligocène à nos jurs et leurs cadres géodinamiques: Données nouvelles et synthèse, *Rev. Geol. Dyn. Geogr. Phys.*, *21*, 41–55.

Benda, L., J. E. Meulenkamp, and R. R. Schmidt (1982), Biostratigraphic correlations in the Eastern Mediterranean Neogene, 6, Correlation between sporomorph, marine microfossil and mammal associations from some Miocene sections of the Ionian islands and Crete (Greece), *Newsl. Stratigr.*, *11*, 83–93.

Berggren, W. A., D. V. Kent, C. C. Swisher III, and M. P. Aubry (1995), A revised Cenozoic geochronology and chronostratigraphy, in *Geochronology, Time Scales, and Global Stratigraphic Correlation*, edited by W. A. Berggren et al., *Spec. Publ. SEPM Soc. Sediment. Geol.*, *54*, 129–212.

Besang, C., F. J. Eckhart, W. Harre, G. Kreuzer, and P. Muller (1977), Radiometrische Alterbestimmung am neogenen Eruptivgesteinen der Türkei, *Geol. Jahrb.*, *25*, 3–36.

Bizon, G. (1967), Contribution a la connaissance der foraminifères planctoniques de l'Épire et des iles ioniennes (Grèce occidentale), thesis, 44 pp., Inst. Fr. du Petrole, Paris.

Bizon, G., and F. Thiébault (1974), Données nouvelles sur l'âge des marbres et quartzites u Taygéte (Péloponnèse neridional, Grèce), *C. R. Acad. Sci., Ser. D*, *278*, 9–12.

Blake, M. C., M. Bonneau, J. Geyssant, J.-R. Kienast, C. Lepvrier, H. Maluski, and D. Papanikolaou (1981), A geologic reconnaissance of the Cycladic blueschist belt, Greece, *Geol. Soc. Am. Bull.*, *92*, 247–254.

Blasband, B., P. Prooijmans, P. Dirks, W. Visser, and S. H. White (1997), A Pan-African core complex in the Sinai, Egypt, *Geol. Mijnbouw*, *76*, 247–266.

Blümor, T., J. Dollinger, M. Knobel, A. Mutter, S. Zarda, and G. Kowalczyk (1994), Plattenkalk series and Kastania phyllites of the Taygetos Mts.: New results on structure and succession, *Bull. Geol. Soc. Greece*, *15*.

Böger, H. (1983), Stratigraphische und tektonische Verknüpfungen kontinentaler Sedimente des Neogens im Ägäis-Raum, *Geol. Rundsch.*, *72*, 771–814.

Böger, H., R. Gersonde, and R. Willman (1974), Das Neogen im Osten der Insel Kos (Ägäis, Dodekanes)?Stratigraphie und Tektonik, *Neus Jahrb. Geol. Palaeontol. Abh.*, *145*, 129–152.

Bonneau, M., and J. R. Kienast (1982), Subduction, collision et schistes blues (Greece), *Bull. Soc. Geol. Fr.*, *24*, 781–791.

Bornovas, I., and T. Rontogianni-Tsiabaou (1983), Geological map of Greece, Inst. of Geol. and Mineral Explor., Athens.

Brauer, R., R. Ittner, and G. Kowalczyk (1980), Ergebnisse der ''Phyllit-Serie'' SE Lakoniens (Peloponnes, Griechenland), *Neus Jahrb. Geol. Palaeontol. Monatsh.*, *1980*, 129–144.

British Petroleum Company (BP) (1971), The geological results of petroleum exploration in western Greece, *Spec. Rep. 10*, Inst. for Geol. and Subsurface Res., Athens.

Brix, M. R., B. Stöckhert, E. Seidel, T. Theye, S. A. Thomson, and M. Küster (2002), Thermobarometric data from a fossil zircon partial annealing zone in high pressure-low temperature rocks of eastern and central Crete, Greece, *Tectonophysics*, *349*, 309–326.

Bröcker, M., and M. Enders (1999), U-Pb zircon geochronology of unusual eclogite-facies rocks from Syros and Tinos (Cyclades, Greece), *Geol. Mag.*, *136*, 111–118.

Bröcker, M., and L. Franz (1998), Rb-Sr isotope studies on Tinos Island (Cyclades, Greece): Additional time constraints for metamorphism, extent of infiltration controlled overprinting and deformational activity, *Geol. Mag.*, *135*, 369–382.

Bröcker, M., H. Kreuzer, A. Matthew, and M. Okrusch (1993), $^{40}Ar/^{39}Ar$ and oxygen isotope studies of polymetamorphism from Tinos Island, Cycladic blueschist belt, Greece, *J. Metamorph. Geol.*, *11*, 223–240.

Buck, W. R., F. Martinez, M. S. Steckler, and J. R. Cochran (1988), Thermal consequences of lithospheric extension: pure and simple, *Tectonics*, *7*, 213–234.

Buick, I. S., and T. J. B. Holland (1989), The P-T-t path associated with crustal extension, Naxos, Cyclades, Greece, in *Evolution of Metamorphic Belts*, edited by J. S. Daly, R. A. Cliff, and B. W. D. Yardley, *Geol. Soc. Spec. Publ.*, *43*, 365–369.

De Mulder, E. F. J. (1975), Microfauna and sedimentary-tectonic history of the Oligo-Miocene of the Ionian Islands and Western Epirus (Greece), *Utrecht Micropal. Bull.*, *13*, 1–139.

Dinter, D. A. (1998), Late Cenozoic extension of the Alpine collisional orogen, Northeastern Greece: Origin of the north Aegean basin, *Geology*, *21*, 45–48.

Dittmar, U., and G. Kowalczyk (1991), Die Metaklastite im Liegenden der Plattenkalk-Karbonate des südlichen Peloponnes, *Z. Dtsch. Geol. Ges.*, *142*, 209–227.

Doutsos, T., I. Koukouvelas, G. Poulimenos, S. Kokkolas, P. Xypolias, and K. Skourlis (2000), An exhumation model of the south Peloponnesus, Greece, *Int. J. Earth Sci.*, *89*, 350–365.

Dremel, G. (1970), Das Miozän von Kephallinia, Ionische Inseln, Griechenland, *Mitt. Bayer. Staatssamml. Palaeontol. Hist. Geol.*, *10*, 3–86.

Finger, F., E. Krenn, G. Riegler, S. Romano, and G. Zulauf (2002), Resolving Cambrian, Carboniferous, Permian and Alpine monazite generations in the polymetamorphic basement of eastern Crete (Greece) by means of the electron microprobe, *Terra Nova*, *14*, 233–240.

Fleury, J. J. (1975), La premier flysch de Pinde témoin de ensemble des événements orogéniques mésozoiques antecretacé supérieureavant affecte les H'llenides internes, *C. R. Acad. Sci.*, *281*, 1459.

Franz, L., M. Okrusch, and M. Bröcker (1993), Polymetamorphic evolution of pre-Alpidic basement rocks on the island of Sikinos (Cyclades, Greece), *Nues. Jahrb. Mineral. Montasch.*, *1993*, 145–162.

Fytikas, M., O. Giuliani, F. Innocenti, G. Merinelli, and R. Mazzuol (1976), Geochronological data on Recent magmatism of the Aegean Sea, *Tectonophysics*, *31*, 29–34.

Fytikas, M., F. Innocenti, N. Kolios, P. Manetti, R. Mazzuoli, G. Poli, F. Rita, and L. Villari (1986), Volcanology and petrology of volcanic products of the island of Milos and neighbouring islets, *J. Volcanol. Geotherm. Res.*, *28*, 297–317.

Gautier, P., and J.-P. Brun (1994), Crustal-scale geometry and kinematics of late-orogenic extension in the central Aegean (Cyclades and Evvia Island), *Tectonophysics*, *238*, 399–424.

Gautier, P., J.-P. Brun, and L. Jolivet (1993), Structure and kinematics of Upper Cenozoic extensional detachment on Naxos and Paros, *Tectonics*, *12*, 1180–1194.

Gautier, P., J.-P. Brun, R. Moriceau, D. Sokoutis, J. Martinod, and L. Jolivet (1999), Timing, kinematics and cause of Aegean extension: A scenario based on a comparison with simple analogue experiments, *Tectonophysics*, *315*, 31–72.

Hagn, H., H. Bergmann, B. Bischoff, K. Braune, G. Dremel, F. Hug, and W. Ott (1967), Zur neogenstratigraphie von Kefallonia und Ithaka, *Giornali Geol.*, *35*, 179–188.

Hatzipanagiotou, K. (1988), Einbindung der obersten Einheit von Rhodos und Karpathos (Griechenland) in den alpidischen Ophiolith-Gürtel, *Neus Jahrb. Geol. Palaeontol. Abh.*, *176*, 395–422.

Hejl, E., H. Riedl, and H. Weingartner (2002), Post-plutonic unroofing and morphogenesis of the Attic-Cycladic complex (Aegea, Greece), *Tectonophysics*, *349*, 37–56.

Henjes-Kunst, F., and H. Kreuzer (1982), Isotopic dating of pre-alpidic rocks from the island of Ios (Cyclades, Greece), *Contrib. Mineral. Petrol*, *80*, 245–253.

Henjes-Kunst, F., R. Altherr, H. Kreuzer, and B. Tauber Hansen (1988), Disturbed U-Th-Pb systematics of young zircons and uranothorites: The case of the Miocene Aegean granitoids (Greece), *Chem. Geol.*, *73*, 125–145.

Hrouda, F. (1982), Magnetic anisotropy of rocks and its applicability in geology and geophysics, *Geophys. Surv.*, *5*, 37–82.

Innocenti, F., N. Kolios, P. Manetti, F. Rita, and L. Villari (1982), Acid and basic late Neogene volcanism in central Aegean Sea: Its nature and geotectonic significance, *Bull. Vulcanol.*, *45*, 87–97.

Institut de Géologie et Recherches du Sous-Sol–Institut Francais du Petrole (IGRS-IFP) (1966), *Étude Géologique de l'Épire (Grèce Nord-Occidentale)*, 306 pp., Ed. Technip, Paris.

Jacobshagen, V. (1986), *Geologie von Griechenland*, pp. 257–279, Borntraeger, Stuttgart, Germany.

Jenkins, D. A. L. (1972), Structural development of western Greece, *AAPG Bull.*, *56*, 128–149.

Jolivet, L., and B. Goffé (2000), Les dômes métamorphiques extensifs dans les chaînes de montagnes: Extension syn-orogénique et post-orogénique, *C. R. Acad. Sci.*, *330*, 739–751.

Jolivet, L., J.-P. Brun, P. Gautier, S. Lallemant, and M. Patriat (1994), 3D-kinematics of extension in the Aegean region from the early Miocene to the Present, insights from the ductile crust, *Bull. Soc. Geol. Fr.*, *165*, 195–209.

Jolivet, L., B. Goffé, P. Monié, C. Truffert-Luxey, M. Patriat, and M. Bonneau (1996), Miocene detachment on Crete and exhumation P-T-t paths of high-pressure metamorphic rocks, *Tectonics*, *15*, 1129–1153.

Jolivet, L., C. Facenna, B. Goffé, E. Burov, and P. Agard (2003), Subduction tectonics and exhumation of high-pressure metamorphic rocks in the Mediterranean orogen, *Am. J. Sci.*, *303*, 353–409.

Jolivet, L., V. Famin, C. Mehl, T. Parra, C. Aubourg, R. Hébert, and P. Philippot (2004a), Progressive strain localization, boudinage and extensional metamorphic complexes: The Aegean Sea case, in *Gneiss Domes in Orogeny*, edited by D. L. Whitney, C. Teyssier, and C. S. Siddoway, *Spec. Pap. Geol. Soc. Am.*, *380*, 185–210.

Jolivet, L., G. Rimmelé, R. Oberhänsli, B. Goffé, and O. Candan (2004b), Correlation of syn-orogenic tectonic and metamorphic events in the Cyclades, the Lycian Nappes and the Menderes Massif: Geodynamic implications, *Bull. Soc. Geol. Fr.*, *175*, 217–238.

Karakitsios, V. (1995), The influence of pre-existing structure and halokinesis on organic matter preservation and thrust system evolution in the Ionian Basin, northwest Greece, *AAPG Bull.*, *79*, 960–980.

Katagas, C., P. Tsolis-Katagas, and E. Baltatzis (1991), Chemical mineralogy and illite crystallinity in low grade metasediments, Zarouchla Group, Northern Peloponnesus, Greece, *Mineral. Petrol.*, *44*, 57–71.

Keay, S., G. Lister, and I. Buick (2001), The timing of partial melting, Barrovian metamorphism and granite intrusion in the Naxos metamorphic core complex, Cyclades, Aegean Sea, Greece, *Tectonophysics*, *342*, 275–312.

Kissel, C., E. Barrier, C. Laj, and T. Q. Lee (1986), Magnetic fabric in "undeformed" marine clays from compressional zones, *Tectonics*, *5*, 183–201.

Kissel, C., C. Laj, A. Poisson, and N. Görür (2003), Paleomagnetic reconstruction of the Cenozoic evolution of the eastern Mediterranean, *Tectonophysics*, *362*, 199–217.

Klein-Helmkamp, U., T. Reinecke, and B. Stöckhert (1995), The aragonite-calcite-transition in LT-HP metamorphic carbonate rocks from S-Evia, Greece: The microstructural and compositional record, *Bochumer Geol. Geotech. Arb.*, *44*, 78–83.

Koepke, J., E. Seidel, and H. Kreuzer (2002), Ophiolites in the southern Aegean Islands Crete, Karpathos and Rhodes: Composition, geochronology and position within the ophiolite belts of the eastern Mediterranean, *Lithos*, *65*, 183–203.

Kornprobst, J., J.-R. Kienast, and J.-C. Vilminot (1979), The high-pressure assemblages at Milos, Greece, *Contrib. Mineral. Petrol*, *69*, 49–63.

Kowalczyk, G., and U. Dittmar (1991), The metamorphics underlying the Plattenkalk carbonates in the Taygetos Mts. (Southern Peloponnese), *Bull. Geol. Soc. Greece*, *25*, 455–467.

Kowalczyk, G., and P. Zügel (1997), Die Vatia-Schichten-Flysch der Plattenkalk-Serie des Peloponnes, *Cour. Forsch. Inst. Senckenberg*, *201*, 259–275.

Krahl, J., G. Kaufmann, H. Kozur, D. Richter, O. Förster, and F. Heinritzi (1983), Neue Daten zur Biostratigraphie und zur tectonischen Lagerung der Phyllit-Gruppe und der Tripali-Gruppe auf der Insel Kreta (Griechenland), *Geol. Rundsch.*, *72*, 1147–1166.

Krahl, J., G. Kaufmann, D. Richter, H. Kozur, I. Möller, O. Förster, F. Heinritzi, and U. Dornsiepen (1986), Neue Fossilfunde in der Phyllit-Gruppe Ostkretas (Griechenland), *Z. Dtsch. Geol. Ges.*, *137*, 523–536.

Kreuzer, H., W. Harre, H. Lenz, I. Wendt, F. Henjes-Kunst, and M. Okrusch (1978), K/Ar und Rb/Sr-Daten von Mineralen aus dem polymetamorphen Kristallin fer Kykladen-Insel Ios (Griechenland), *Fortschr. Mineral.*, *56*, 69–70.

Lensky, N., D. Avigad, Z. Garfunkel, and B. W. Evans (1997), The tectono-metamorphic evolution of blueschists in South Evia, Hellenide orogenic belt (Greece), paper presented at Israel Geological Society Annual Meeting, Kfar Giladi, Israel.

Linssen, J. H. (1991), Properties of Pliocene sedimentary geomagnetic reversal records from the Mediterranean, *Geol. Ultraiectina*, *80*, 1–231.

Lips, A. L. W. (1998), Temporal constraints on the kinematics of the destabilization of an orogen: Syn- to post-orogenic extensional collapse of the northern Aegean region, *Geol. Ultraiectina*, *166*, 1–224.

Lips, A. L. W., S. H. White, and J. R. Wijbrans (2000), Middle-Late Alpine thermotectonic evolution of the southern Rhodope Massif, Greece, *Geodin. Acta*, *13*, 281–292.

Lister, G. S., and A. Raouzaios (1996), The tectonic significance of a porphyroblastic blueschist facies overprint during Alpine orogenesis: Sifnos, Aegean Sea, Greece, *J. Struct. Geol.*, *18*, 1417–1435.

Lister, G., G. Banga, and A. Feenstra (1984), Metamorphic core complexes of Cordilleran type in the Cyclades, Aegean Sea, Greece, *Geology*, *12*, 221–225.

Lourens, L. J., F. J. Hilgen, J. Laskar, N. J. Shackleton, and D. Wilson (2005), The Neogene period, in *A Geologic Time Scale 2004*, edited by F. M. Gradstein, J. G. Ogg, and A. G. Smith, pp. 409–440, Cambridge Univ. Press, New York.

Maluski, H., P. Vergely, D. Bavay, P. Bavay, and G. Katsikatsos (1981), $^{39}Ar/^{40}Ar$ dating of glaucophanes and phengites in southern Euboa (Greece): Geodynamic implications, *Bull. Soc. Geol. Fr.*, *5*, 469–476.

Manutsoglu, M. (1990), Tektonik und Metamorphose der Plattenkalk-Serie im Taygetos (Peloponnes, Griechenland), *Berlin. Geowiss. Abh.*, *129*, 1–82.

Matthews, A., and M. Schliestedt (1984), Evolution of the blueschist and greenschist facies rocks of Sifnos, Cyclades, Greece: A stable isotope study of subduction-related metamorphism, *Contrib. Mineral. Petrol.*, *88*, 150–163.

McKenzie, D. (1978), Some remarks on the development of sedimentary basins, *Earth Planet. Sci. Lett.*, *40*, 25–32.

Meco, S., and S. Aliaj (2000), *Geology of Albania*, 246 pp., Gebrueder Borntraeger, Berlin.

Meissner, B. (1976), Das Neogen von Ost-Samos: Sedimentationsgeschichte und Korrelation, *Neus Jahrb. Geol. Palaeontol. Monatsh.*, *152*, 161–176.

Meulenkamp, J. E. (1982), On the pulsating evolution of the Mediterranean, *Episodes*, *1982*, 13–16.

Mpsokos, E., and V. Pedikatsis (1984), Petrology of glaucophane metagabbros and related rocks from Samos, Aegean Island (Greece), *Neus Jahrb. Mineral. Abh.*, *149*, 43–63.

Okrusch, M., and M. Bröcker (1990), Eclogite facies rocks in the Cycladic blueschist belt, Greece: A review, *Eur. J. Mineral.*, *2*, 451–478.

Okrusch, M., E. Seidel, and E. N. Davis (1978), The assemblage jadeite-quartz in the glaucophane rocks of Sifnos (Cyclades Archipelago, Greece), *Neus Jahrb. Mineral. Abh.*, *132*, 284–308.

Panagos, A. G., G. G. Pe, D. J. W. Piper, and C. N. Kotopouli (1979), Age and stratigraphic subdivision of the Phyllite series, Krokee region, Peloponnese, Greece, *Neus Jahrb. Geol. Palaeontol. Monatsh.*, *3*, 182–190.

Papanikolaou, D., V. Lykoussis, G. Chronis, and P. Pavlakis (1988), A comparative study of neotectonic basins across the Hellenic Arc: The Messiniakos, Argolikos and Southern Evoikos Gulfs, *Basin Res.*, *1*, 167–176.

Peeters, F. J. C., R. P. Hoek, H. Brinkhuis, M. Wilpshaar, P. L. De Boer, W. Krijgsman, and J. E. Meulenkamp (1998), Differentiating glacio-eustacy and tectonics: A case study involving dinoflagellate cysts from the Eocene-Oligocene transition of the Pindos Foreland Basin (NW Greece), *Terra Nova*, *10*, 245–249.

Pe-Piper, G. (1982), Geochemistry, tectonic setting and metamorphism of mid-Triassic volcanic rocks of Greece, *Tectonophysics*, *85*, 253–272.

Reinecke, T. (1986), Phase relationships of sursassite and other Mn-silicates in highly oxidised low-grade high-pressure rocks from Evvia and Andros Islands, Greece, *Contrib. Mineral. Petrol.*, *94*, 110–126.

Reinecke, T., R. Altherr, B. Hartung, K. Hatzipanagiotou, H. Kreuzer, W. Harre, H. Klein, J. Keller, E. Geenen, and H. Böger (1982), Remnants of Late Cretaceous high temperature belt on the island of Anáfi (Cyclades, Greece), *Neus Jahrb. Mineral. Abh.*, *145*, 157–182.

Richter, D., I. Mariolakos, and H. Risch (1978), The main flysch stages of the Hellenides, in *Alps, Apennines, Hellenides, Inter-Union Comm. on Geodyn. Sci. Rep.*, vol. 38, edited by H. Closs, D. Roeder, and K. Schmidt, pp. 434–438, Schweizerbart, Stuttgart, Germany.

Ricou, L.-E., J.-P. Burg, I. Godfriaux, and Z. Ivanov (1998), Rhodope and Vardar: The metamorphic and the olistostromic paired belts related to the Cretaceous subduction under Europe, *Geodyn. Acta*, *11*, 285 – 309.

Ring, U., and P. W. Layer (2003), High-pressure metamorphism in the Aegean, eastern Mediterranean: Underplating and exhumation from the Late Cretaceous until the Miocene to Recent above the retreating Hellenic subduction zone, *Tectonics*, *22*(3), 1022, doi:10.1029/2001TC001350.

Ring, U., and T. Reishmann (2002), The weak and superfast Cretan detachment, Greece: Exhumation at subduction rates in extruding wedges, *J. Geol. Soc. London*, *159*, 225 – 228.

Ring, U., S. Laws, and M. Bernet (1999), Structural analysis of a complex nappe sequence and late-orogenic basins from the Aegean Island of Samos, *J. Struct. Geol.*, *21*, 1575 – 1601.

Ring, U., P. W. Layer, and T. Reischmann (2001), Miocene high-pressure metamorphism in the Cyclades and Crete, Aegean Sea, Greece: Evidence for large-magnitude displacement on the Cretan detachment, *Geology*, *29*, 395 – 398.

Ring, U., S. N. Thomson, and M. Bröcker (2003), Fast extension but little exhumation: The Vari detachment in the Cyclades, Greece, *Geol. Mag.*, *3*, 245 – 252.

Robert, U., and J. M. Cantagrel (1977), Le volcanism basaltique dans le Sud-Est de la mer Egée: Données géochronologiques et relations avex la tectonique, paper presented at 6th Colloquium on the Geology of the Aegean Region, Inst. of Geol. and Min. Explor., Athens.

Robertson, A. H. F. (2000), Mesozoic-Tertiary tectonic-sedimentary evolution of a South Tethyan oceanic basin and its margins in southern Turkey, edited by E. Bozkurt, J. A. Winchester, and J. D. A. Paper, *Geol. Soc. Spec. Publ.*, *173*, 97 – 138.

Rosenbaum, G., D. Avigad, and M. Sanchez-Gomez (2002), Coaxial flattening at deep levels of orogenic belts: Evidence from blueschists and eclogites on Syros and Sifnos (Cyclades, Greece), *J. Struct. Geol.*, *24*, 1451 – 1462.

Sánchez-Gómez, M., D. Avigad, and A. Heimann (2002), Geochronology of clasts in allochthonous Miocene sedimentary sequences on Mykonos and Paros Islands: Implications for back-arc extension in the Aegean Sea, *J. Geol. Soc. London*, *159*, 45 – 60.

Schliestedt, M., and A. Matthews (1987), Transformation of blueschist to greenschist facies rocks as a consequence of fluid infiltration, Sifnos (Cyclades), Greece, *Contrib. Mineral. Petrol*, *97*, 237 – 250.

Schliestedt, M., R. Altherr, and A. Matthews (1987), Evolution of the Cycladic crystalline complex: Petrology, isotope chemistry, ad geochronology, in *Chemical Transport in Metasomatic Processes*, edited by H. C. Helgeson, *Nato Sci. Ser., Ser. C 218*, 389 – 428.

Seidel, E., M. Okrush, H. Kreuzer, H. Raschka, and W. Harre (1981), Eo-alpine metamorphism in the uppermost unit of the Cretan Nappe-PilēPetrology and geochronology, part 1. The Lendas area (Asteroussia Mountains), *Contrib. Mineral. Petrol.*, *57*, 259 – 275.

Seidel, E., H. Kreuzer, and W. Harre (1982), A late Oligocene/early Miocene high pressure belt in the External Hellenides, *Geol. Jahrb., Reihe E*, *23*, 165 – 206.

Sen, S., and J.-P. Valet (1986), Magnetostratigraphy of late Miocene continental deposits in Samos, Greece, *Earth Planet. Sci. Lett.*, *80*, 167 – 174.

Shaked, Y., D. Avigad, and Z. Garfunkel (2000), Alpine high-pressure metamorphism at the Almyropotamos window (southern Evia, Greece), *Geol. Mag.*, *137*, 367 – 380.

Smith, P. E., D. York, Y. Chen, and N. M. Evensen (1996), Single crystal $^{40}Ar/^{39}Ar$ dating of a late Quaternary paroxysm on Kos, Greece: Concordance of terrestrial and marine ages, *Geophys. Res. Lett.*, *23*, 3047 – 3050.

Sotiropoulos, S., E. Kamberis, M. V. Triantaphyllou, and T. Doutsos (2003), Thrust sequences in the central part of the External Hellenides, *Geol. Mag.*, *140*, 661 – 668.

Stöckhert, B., M. Wachmann, M. Kuester, and S. Bimmerman (1999), Low-effective viscosity during high-pressure metamorphism due to dissolution precipitation creep: The record of HP-LT metamorphic carbonates and siliciclastic rocks from Crete, *Tectonophysics*, *303*, 299 – 319.

Stoykova, K., P. Avramidis, and A. Zelilidis (2003), Calcareous nannofossil stratigraphy of Tertiary submarine fan deposits from the Klematia-Paramythia Basin (Pindos foreland basin, western Greece), *Geol. Carpathica*, *54*, 107 – 118.

Tarling, D. H., and F. Hrouda (1993), *The Magnetic Anisotropy of Rocks*, 217 pp., CRC Press, Boca Raton, Fla.

Theye, T., and E. Seidel (1991), Petrology of low-grade high-pressure metapelites from the External Hellenides (Crete, Peloponnese): A case study with attention to sodic minerals, *Eur. J. Mineral.*, *3*, 343 – 366.

Theye, T., E. Seidel, and O. Vidal (1992), Carpholite, sudoite and chloritoid in low-grade high-pressure metapelites from Crete and the Peloponnese, *Eur. J. Mineral.*, *4*, 487 – 507.

Thiébault, F. A. T. C. (1979), Stratigraphie de la série des calcschistes et merbres (''Plattenkalk'') en fenêtre dans les massifs du Taygète et du Paron (Péloponnèse-Grèce), in *Proceedings of the VI Colloquium of the Geology of the Aegean Region*, pp. 691 – 701, Inst. of Geol. and Min. Explor., Athens.

Thomson, S. N., B. Stöckhert, and M. R. Brix (1998), Thermochronology of the high-pressure metamorphic rocks of Crete, Greece: Implications for the speed of tectonic processes, *Geology*, *26*, 259 – 262.

Thomson, S. N., B. Stöckhert, and M. R. Brix (1999), Miocene high-pressure metamorphic rocks of Crete, Greece: Rapid exhumation by buoyant escape, in *Exhumation Processes: Normal faulting, Ductile Fow and Erosion*, edited by U. Ring et al., *Geol. Soc. Spec. Publ.*, *154*, 87 – 107.

Tomaschek, F., A. K. Kennedy, I. M. Villa, M. Lagos, and C. Ballhaus (2003), Zircons from Syros, Cyclades, Greece—Recrystallization and mobilization of zircon during high-pressure metamorphism, *J. Petrol.*, *44*, 1977 – 2002.

Trotet, F., L. Jolivet, and O. Vidal (2001), Tectonometamorphic evolution of Syros and Sifnos islands (Cyclades, Greece), *Tectonophysics*, *338*, 179 – 206.

Van Couvering, J. A., and J. A. Miller (1971), Late Miocene marine and non-marine time scale in Europe, *Nature*, *230*, 569 – 573.

Van der Maar, P. A., and J. B. A. Jansen (1983), The geology of the polymetamorphic complex of Ios, Cyclades, Greece and its significance for the Cycladic Massif, *Geol. Rundsch.*, *72*, 283 – 299.

Van der Zwaan, G. J., F. J. Jorissen, and H. C. De Stigter (1990), The depth dependency of planktonic/benthonic foraminiferal ratios: Constraints and applications, *Mar. Geol.*, *95*, 1 – 16.

van Hinsbergen, D. J. J. (2004), The evolving anatomy of a collapsing orogen, *Geol. Ultraiectina*, *243*, 280 pp.

van Hinsbergen, D. J. J., E. Snel, S. A. Garstman, M. Marunteanu, C. G. Langereis, M. J. R. Wortel, and J. E. Meulenkamp (2004), Vertical motions in the Aegean volcanic arc: Evidence for rapid subsidence preceding in situ volcanism, *Mar. Geol.*, *209*, 329 – 345.

van Hinsbergen, D. J. J., C. G. Langereis, and J. E. Meulenkamp (2005a), Revision of the timing, magnitude and distribution of Neogene rotations in the western Aegean region, *Tectonophysics*, *396*, 1 – 34.

van Hinsbergen, D. J. J., T. J. Kouwenhoven, and G. J. van der Zwaan (2005b), Palaeobathymetry in the backstripping procedure: Correction for oxygenation effects on depth estimates, *Palaeogeogr. Palaeoclimatol. Palaeoecol.*, in press.

Vincente, J. C. (1970), Etude géologique de l'île de Gavdos (Grèce), la plus méridonale de lÉurope, *Bull. Soc. Geol. Fr.*, *7*, 481 – 495.

Wachmann, M. (1997), Die strukturelle entwicklung hochdruckmetamorpher Karbonatgesteine bei Agios Theodori, S. W. Kreta, *Bochumer Geol. Geotech. Arb.*, *48*, 146 pp.

Weidmann, M., N. Solounias, R. E. Drake, and G. H. Curtis (1984), Neogene stratigraphy of the Eastern Basin, Samos Island, Greece, *Geobios*, *17*, 477 – 490.

Wijbrans, J. R., and I. McDougall (1988), Metamorphic evolution of the Attic Cycladic metamorphic belt on Naxos (Cyclades, Greece) utilizing $^{40}Ar/^{39}Ar$ age spectrum measurements, *J. Metamorph. Geol.*, *6*, 571 – 594.

Wijbrans, J. R., J. D. van Wees, R. A. Stephenson, and S. A. P. L. Cloetingh (1993), Pressure-temperature-time evolution of the high-pressure metamorphic complex of Sifnos, Greece, *Geology*, *21*, 443 – 446.

Willmann, R. (1983), Neogen und jungtertiäre Enwicklung der Insel Kos (Ägäis, Griechenland), *Geol. Rundsch.*, *72*, 815 – 860.

Wilpshaar, M. (1995), Applicability of dinoflagellate cyst stratigraphy to the analysis of passive and active tectonic settings, *Geol. Ultraiectina.*, *134*.

Xypolias, P., and I. K. Koukouvelas (2001), Kinematic vorticity and strain rate patterns associated with ductile extrusion in the Chelmos Shear Zone (External Hellenides, Greece), *Tectonophysics*, *338*, 59 – 77.

Xypolias, P., S. Kokkalas, and K. Skourlis (2003), Upward extrusion and subsequent transpression as a possible mechanism for the exhumation of HP/LT rocks in Evia Island (Aegean Sea, Greece), *J. Geodyn.*, *35*, 303 – 332.

Zulauf, G., G. Kowalczyk, J. Krahl, R. Petschick, and S. Schwanz (2002), The tectonometamorphic evolution of high-pressure low-temperature metamorphic rocks of eastern Crete, Greece: Constraints from microfabrics, strain, illite crystallinity an paleodifferential stress, *J. Struct. Geol.*, *24*, 1805 – 1828.

J. E. Meulenkamp and M. J. R. Wortel, Vening Meinesz Research School of Geodynamics, Department of Earth Sciences, Utrecht University, Budapestlaan 4, NL-3584, CD Utrecht, Netherlands.

D. J. J. van Hinsbergen, Department of Geology, University of Leicester, University Road, Leicester LE1 7RH, UK. (dvh1@le.ac.uk)

W. J. Zachariasse, Institute for Paleoenvironments and Paleoclimate Utrecht, Department of Earth Sciences, Utrecht University, Budapestlaan 4, NL-3584 CD Utrecht, Utrecht, Netherlands.

Figure 9. Time chart for the Cycladic islands, Evia, and Attica, in which the metamorphic history of the Cycladic blueschist unit is summarized. Note that most ages represent cooling ages, postdating the peak metamorphic conditions of the dated mineral. Reference key is as follows: 1, *Altherr et al.* [1976]; 2, *Altherr et al.* [1979]; 3, *Altherr et al.* [1982]; 4, *Altherr et al.* [1988]; 5, *Allen et al.* [1999]; 6, *Andriessen et al.* [1979]; 7, *Andriessen et al.* [1987]; 8, *Andriessen*, 1991]; 9, *Angelier et al.* [1977]; 10, *Aubourg et al.* [2000]; 11, *Avigad and Garfunkel* [1989]; 12, *Avigad et al.* [1998]; 13, *Baldwin and Lister* [1998]; 14, *Bellon et al.* [1979]; 15, *Besang et al.* [1977]; 16, *Blake et al.* [1981]; 17, *Böger et al.* [1974]; 18, *Böger* [1983]; 19, *Bonneau and Kienast* [1982]; 20, *Bröcker et al.* [1993]; 21, *Bröcker and Franz* [1998]; 22, *Bröcker and Enders* [1999]; 23, *Franz et al.* [1993]; 24, *Fytikas et al.* [1976]; 25, *Fytikas et al.* [1986]; 26, *Gautier et al.* [1993]; 27, *Gautier and Brun* [1994]; 28, *Hejl et al.* [2002]; 29, *Henjes-Kunst and Kreuzer* [1982]; 30, *Henjes-Kunst et al.* [1988]; 31, *Innocenti et al.* [1982]; 32, *Keay et al.* [2001]; 33, *Klein-Helmkamp et al.* [1995]; 34, *Kornprobst et al.* [1979]; 35, *Kreuzer et al.* [1978]; 36, *Lensky et al.* [1997]; 37, *Lister and Raouzaios* [1996]; 38, *Maluski et al.* [1981]; 39, *Matthews and Schliestedt* [1984]; 40, *Meissner* [1976]; 41, *Mpsokos and Pedikatsis* [1984]; 42, *Okrusch et al.* [1978]; 43, *Okrusch and Bröcker* [1990]; 43, *Reinecke* [1986]; 44, *Ring and Layer* [2003]; 45, *Ring et al.* [2003]; 46, *Robert and Cantagrel* [1977]; 47, *Rosenbaum et al.* [2002]; 48, *Sánchez-Gómez et al.* [2002]; 49, *Schliestedt et al.* [1987]; 50, *Schliestedt and Matthews* [1987]; 51, *Sen and Valet* [1986]; 53, *Shaked et al.* [2000]; 54, *Smith et al.* [1996]; 55, *Tomaschek et al.* [2003]; 56, *Trotet et al.* [2001]; 57, *Van Couvering and Miller* [1971]; 58, *Van der Maar and Jansen* [1983]; 59, *van Hinsbergen et al.* [2004]; 60, *Weidmann et al.* [1984]; 61, *Willmann* [1983]; 62, *Wijbrans and McDougall* [1988]; 63, *Wijbrans et al.* [1993].

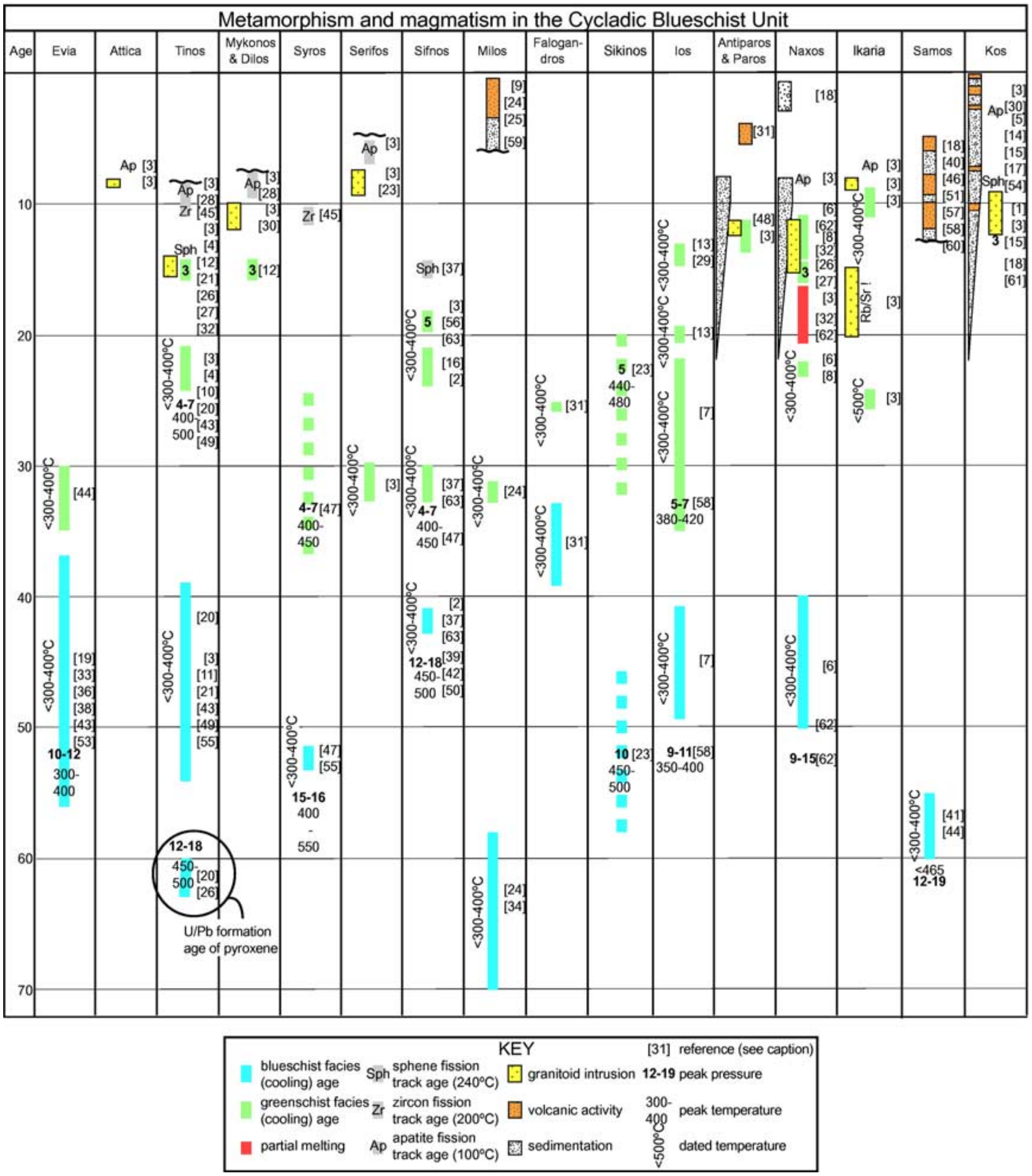
Metamorphism and magmatism in the Cycladic Blueschist Unit
Age
Evia
Attica
Tinos
Mykonos & Dilos
Syros
Serifos
Sifnos
Milos
Falogandros
Sikinos
Ios
Antiparos & Paros
Naxos
Ikaria
Samos
Kos
U/Pb formation age of pyroxene
KEY
blueschist facies (cooling) age
greenschist facies (cooling) age
partial melting
sphene fission track age (240°C)
zircon fission track age (200°C)
apatite fission track age (100°C)
granitoid intrusion
volcanic activity
sedimentation
[31] reference (see caption)
12-19 peak pressure
300-400 peak temperature
<500°C dated temperature

Figure 9